Geometry and kinematic evolution of a long-living foreland structure inferred from field data and cross section balancing, the Sainte-Victoire System, Provence, France

N. Espurt, J.C. Hippolyte, Marianne Saillard, O Bellier

Geometry and kinematic evolution of a long-living foreland structure inferred from field data and cross section balancing, the Sainte-Victoire System, Provence, France

Nicolas Espurt,[1] Jean-Claude Hippolyte,[1] Marianne Saillard,[2] and Olivier Bellier[1]

Received 11 July 2011; revised 7 June 2012; accepted 27 June 2012; published 15 August 2012.

[1] The Sainte-Victoire System (SVS) is a key area to understand how the shortening is accommodated in outer foreland of the Pyrenean-Provence orogen between Late Cretaceous and Eocene. Structural data, growth strata and fault slip analysis, and four balanced cross sections are used to decipher the along-strike geometry, deformational characteristics and kinematics of the SVS. The SVS is divided into two structural domains separated by a regional relay zone: the eastern domain is governed by a N-vergent thin-skinned tectonic style above Triassic series and the western domain, by a mixed S-vergent thick- and thin-skinned tectonic style with tectonic inversion of Late Paleozoic-Triassic half grabens. Growth strata indicate that the eastern SVS grew during Danian as a result of shortening transfer from the southern Arc Basin. In contrast, the western SVS is an independent structure which has recorded the early stage (~83 Ma) of shortening and focused continuous deformation during ~40 Myr. The shallow N-S shortening is ~5 km (~25%) and ~8 km (~34%) in the western and eastern SVS, respectively. At a regional scale, the tectonic inversion of the SVS and the Arc Basin recorded a deep shortening of the order of 15–18 km (~34%). Although the shortening magnitude of the SVS remains small, other structures similar to the SVS were synchronously active across foreland basin, suggesting a significant amount of cumulated shortening. This outer foreland shortening may account for a non-negligible amount of deformation at the Pyrenean-Provence orogen scale.

Citation: Espurt, N., J.-C. Hippolyte, M. Saillard, and O. Bellier (2012), Geometry and kinematic evolution of a long-living foreland structure inferred from field data and cross section balancing, the Sainte-Victoire System, Provence, France, *Tectonics*, *31*, TC4021, doi:10.1029/2011TC002988.

1. Introduction

[2] The tectono-sedimentary evolution of fold-and-thrust belts can be influenced by foreland structural inheritances [e.g., *McClay and Buchanan*, 1992; *Coward*, 1996; *Roure and Colletta*, 1996; *Butler et al.*, 2006; *Mora et al.*, 2006]. For example, inherited rift-related structures with basement normal faults may preferentially accommodate shortening in the outer region of foreland in response to the far-field transmission of orogenic stresses [*Coward*, 1996; *Lacombe and Mouthereau*, 2002; *Hilley et al.*, 2005]. This outer foreland thick-skinned thrusting may record the early stage of shortening and leads to the formation of isolated uplift zones and localized syntectonic depocenters [*McClay*, 1989; *Hain et al.*, 2011]. The orientation of the inherited normal faults, respectively to the strike of subsequent shortening, and the expulsion of the thick initial sedimentary cover may lead to the development of transverse structures [e.g., *Marshak and Wilkerson*, 1992; *Macedo and Marshak*, 1999]. When inversion geometries and compression direction have been clearly identified, cross section balancing can be properly used to restore inverted basins to their initial stages and estimate the amount and rate of shortening [*Coward*, 1996].

[3] The Late Cretaceous-Eocene Pyrenean foreland of Provence is composed of an array of multidirectional compressional structures, oriented from N010°E to N120°E, with highly disparate space-time patterns of deformation and sedimentation (Figure 1a). This structural framework reflects basement and stratigraphic heterogeneities of the Eurasian margin inherited from the Paleozoic and Mesozoic times [e.g., *Tempier*, 1987]. In this paper, we present the results of a detailed fieldwork in the Sainte-Victoire System and adjacent Arc and Rians Basins located in the northern part of the Pyrenean foreland of Provence (Figure 1 and Figure 2). The strong erosional level and weak vegetal coverage of the study area provide an extremely good cross-sectional exposure of geological structures. Structural analysis benefits

[1]Aix-Marseille Université, CNRS, CEREGE UMR 7330, Aix-en-Provence, France.
[2]Géoazur, Université Nice Sophia-Antipolis, Centre National de la Recherche Scientifique (UMR 7329), Observatoire de la Côte d'Azur, La Darse, Villefranche-sur-Mer Cedex, France.

Corresponding author: N. Espurt, Aix-Marseille Université, CNRS, CEREGE UMR 7330, Technopôle Environnement Arbois-Méditerranée, B.P. 80, FR-13545 Aix-en-Provence CEDEX 4, France. (espurt@cerege.fr)

0278-7407/12/2011TC002988

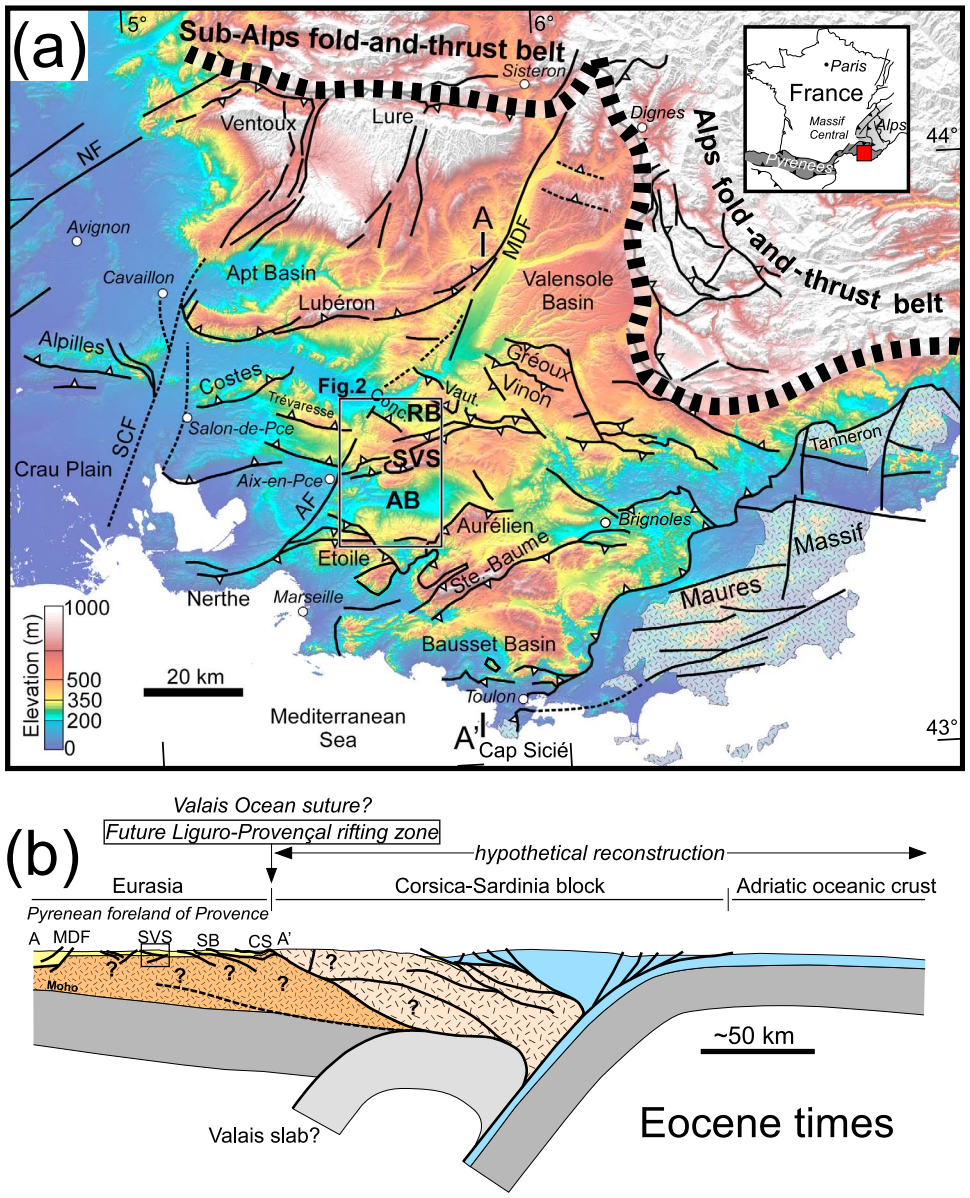

Figure 1. (a) Physiographic map of the Pyrenean/Alpine foreland of Provence. The base map is produced using elevation data from NASA (National Aeronautics and Space Administration) 30 m ASTER (Advanced Spaceborne Thermal Emission and Reflection Radiometer) GDEM (Global Digital Elevation Model). Dashed black line shows the southeastern Alpine thrust front. Dashed areas correspond to the basement rock of the Maures Massif and Tanneron. Location of Figure 2 is indicated by a black frame. (b) Proposed lithospheric scale cross section across the Pyrenean belt of Provence and Corsica-Sardinia block in the Eocene times (modified from *Lacombe and Jolivet* [2005]). A-A′ Provence segment of the cross section is shown on Figure 1a (modified from *Tempier* [1987]). NF: Nîmes fault. SCF: Salon-Cavaillon fault. AF: Aix-en-Provence fault. MDF: Middle Durance fault. SVS: Sainte-Victoire System. RB: Rians Basin. AB: Arc Basin. SB: Sainte-Baume. CS: Cap Sicié.

from outcrops of Mesozoic and Cenozoic deposits, and in particular of Late Cretaceous to Paleocene growth strata accumulation [e.g., *Leleu et al.*, 2005, 2009]. The precise study of the geometry, distribution and ages of growth strata deposits is a key to understand the kinematics of folding and faulting and the timing of deformation [e.g., *Suppe et al.*, 1992].

[4] The Sainte-Victoire System is a widespread dissected feature of Provence whose back thrust behavior and complex along-strike variations in terms of structural architecture and development of syntectonic sedimentary fills are still under debate (Figure 2). Using regional balanced cross sections, *Tempier* [1987] and *Biberon* [1988] suggested that the Sainte-Victoire System corresponds to a N-vergent fault-propagation fold detached above Triassic evaporites. The S-vergent subordinate back-thrusts that propagate through the backlimb, would result in local flexure in the foreland. Based on SPOT imagery and field data, *Chorowicz et al.*

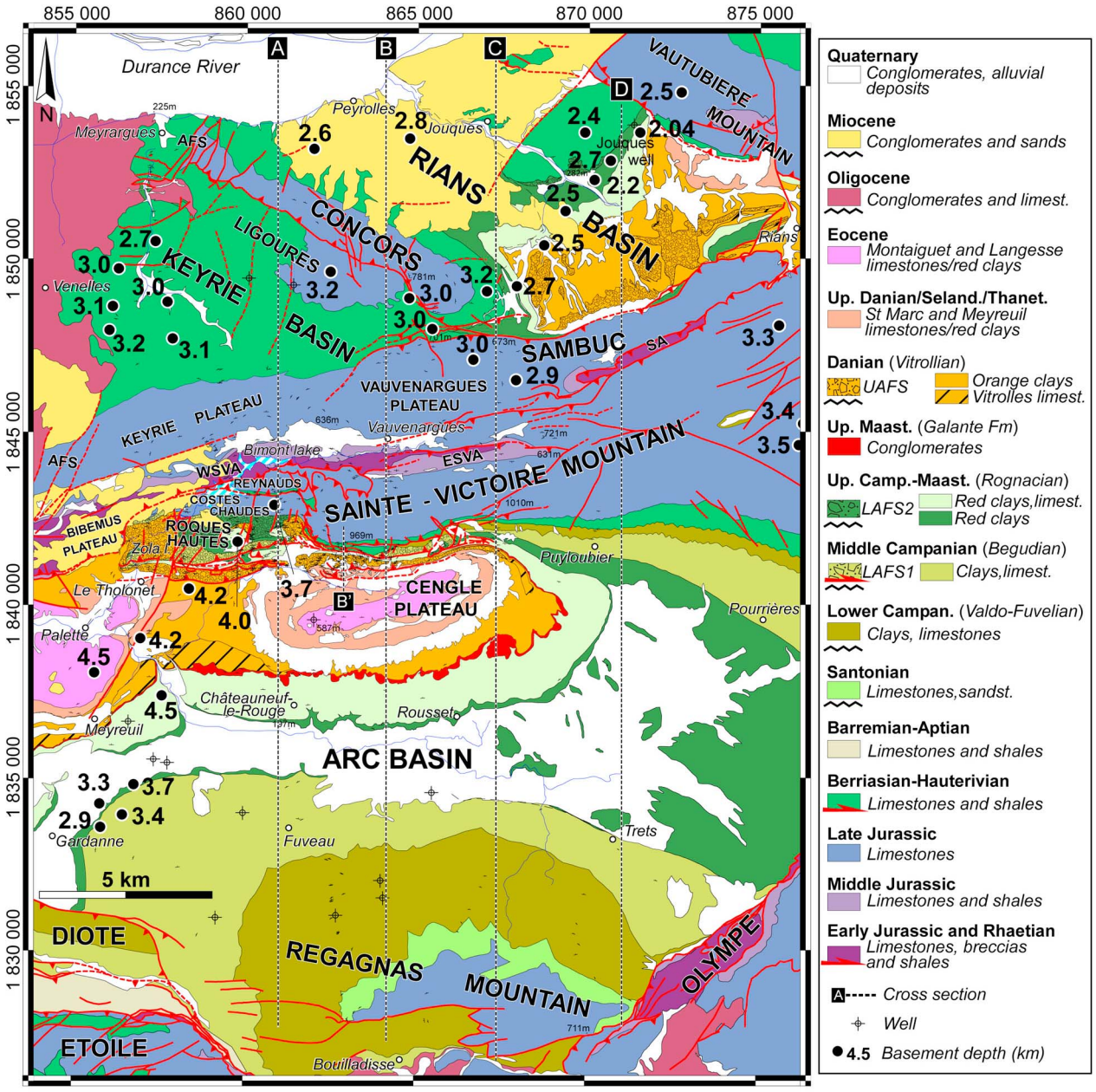

Figure 2. Geologic map of the study area based on field mapping (Sainte-Victoire System area) and published map of BRGM (Aix-en-Provence and Pertuis 1:50 000 maps). Coordinate system is Lambert 2, Paris system (meters). Locations of cross sections A, B, B′, C and D are shown (Figures 4, 8, and 14). Black circles with numbers correspond to depth (km bsl) of the basement rock-sedimentary cover interface inferred from geophysical data [*Biberon*, 1988]. WSVA: western Sainte-Victoire anticline. ESVA: eastern Sainte-Victoire anticline. SA: Sambuc anticline. AFS: Aix fault system. LAFS1 (lower alluvial fan system 1), LAFS2 (lower alluvial fan system 2), and UAFS (upper alluvial fan system) in the sense of *Leleu et al.* [2005].

[1989] interpreted the structure as associated with the structural inversion of "*en échelon*" Early Jurassic normal faults. On the basis of sand-box analog models, *Roure and Colletta* [1996] interpret the structure as a thin-skinned "pop-up" structure within the sedimentary cover, which would accommodate thick-skinned inversion of a deep Permian basin localized below the Arc Basin. More recently, *Ricour et al.* [2005] speculated that the Sainte-Victoire Mountain structure corresponds to a recent horst bounded by subvertical faults.

[5] On the basis of structural data, growth strata and fault slip analysis, and the construction of a series of four balanced and restored cross sections, this paper aims at deciphering the structural architecture, temporal distribution and propagation of the deformation of the Sainte-Victoire System, and syntectonic sedimentary filling of the adjacent Arc and Rians Basins during Late Cretaceous to Eocene

Pyrenean compression. The results yield new insights into the role of inherited basement structures on the general interpretation of the kinematic evolution of the Pyrenean foreland thrust system of Provence during the collision between Eurasia and the Corsica-Sardinia block (Figure 1b).

2. Geological Setting

[6] The Provence region is located in southeastern France at the transition between the Pyrenees and Alps belts (Figure 1a). The Provence structural framework results from two superimposed contractional periods: Late Cretaceous to Eocene corresponding to the Pyrenean compression [e.g., *Lacombe and Jolivet*, 2005] and Miocene to present corresponding to the Alpine compression [e.g., *Bergerat*, 1987; *Champion et al.*, 2000]. These two compressional periods are separated by an Oligocene extensional period with N- and NE-trending structures related to the West European rifting, then to the Liguro-Provencal rifting of the western Mediterranean [*Hippolyte et al.*, 1993; *Gattacceca et al.*, 2007].

[7] E- to SE-trending folds and thrusts (e.g., Nerthe, Alpilles, Costes, Trévaresse, Lubéron, Ventoux-Lure, Concors, Vautubière, Sainte-Victoire Mountain, Etoile, Olympe/Aurélien, Sainte-Baume structures) and regional NNE-trending strike-slip faults (e.g., Nîmes, Salon-Cavaillon, Aix-en-Provence, Middle Durance faults) form the Pyrenean fold-and-thrust belt of Provence (Figure 1a) [*Tempier and Durand*, 1981], and result from the northward subduction of the Valais slab and the collision between the Corsica-Sardinia block and Eurasia during Late Cretaceous to Eocene (Figure 1b) [*Arthaud and Seguret*, 1981; *Lacombe and Jolivet*, 2005; *Schettino and Turco*, 2011]. These structures are commonly interpreted to be inherited from post-Hercynian and Triassic to Late Jurassic rifting associated with the opening of the Tethys Ocean, and during Early Cretaceous rifting of the Valais Ocean related to the opening of the central Atlantic Ocean [*Graciansky and Lemoine*, 1988; *Schettino and Turco*, 2011]. Some Pyrenean structures have been reactivated during E- and SE-trending Oligocene extensional periods (Nîmes, Middle Durance and Aix-en-Provence faults) and N- to NE-trending Miocene to present-day Alpine compression (e.g., Ventoux-Lure, Lubéron and Trévaresse thrusts, and Nîmes, Salon-Cavaillon, Middle Durance faults; Figure 1a) [*Baroux et al.*, 2003; *Guignard et al.*, 2005; *Chardon and Bellier*, 2003; *Terrier et al.*, 2008; *Molliex et al.*, 2011].

2.1. Structures of the Study Area

[8] The study area belongs to the eastern Provence area, east of the Middle Durance/Aix-en-Provence fault system, and north of the Etoile-Aurélien thrust systems (Figure 1a). It comprises three major tectonic units briefly described hereafter: the southern Arc Basin, the central Sainte-Victoire System, and the northern Rians and Kyerié Basins (Figure 2).

2.1.1. Arc Basin

[9] The Arc Basin is a large E-trending 30 km-long, 15 km-wide syncline (Figure 2). It consists predominantly of ~3 km-thick Upper Cretaceous continental sediments accumulated on top of Jurassic series and locally covered by Cenozoic sediments. The syncline is asymmetric, with a long gently dipping southern flank, bounded in the south by Regagnas Mountain, an ESE-trending antiformal structure cored by a thick package of Late Jurassic limestones. The northern flank of the syncline, is shorter and steeper than the southern flank and bounded by the Sainte-Victoire System. In the core of the syncline, the Cengle Plateau is characterized by flat-lying Paleocene-Eocene strata (Figure 2).

2.1.2. Sainte-Victoire System

[10] The Sainte-Victoire System is an E-trending 25 km-long, 7 km-wide structure (Figure 2). The thrust system has significant along-strike variations, and can be divided into two oppositely verging domains: the western and the eastern Sainte-Victoire System [e.g., *Chorowicz et al.*, 1989; *Roure and Colletta*, 1996]. The western Sainte-Victoire System is an overall antiformal structure mainly constituted by Jurassic rocks (~1500 m), and a thinner Cretaceous cover (~500 m), overthrusted southwards on top of the Arc syncline. The basal thrust of the Sainte-Victoire System is a curve-shaped feature which branches westward into the Reynauds, Costes Chaudes and Roques Hautes imbricate units. The western outcrops of this system are strongly eroded (Bibémus Plateau) and unconformably overlain by Miocene marine series. The eastern Sainte-Victoire System consists of two "*en echelon*" anticlines mainly constituted by Jurassic rocks: the eastern Sainte-Victoire and Sambuc anticlines (Figure 2), characterized by N-vergent thrusting toward the Rians Basin [*Chorowicz et al.*, 1989].

2.1.3. Rians and Kyerié Basins

[11] The northern flank of the Sainte-Victoire System is characterized by SE-trending structures. The Rians Basin is a 10 km-long, 6 km-wide syncline (Figure 2). It is overthrusted by the Vautubière Mountain anticline to the northeast and the Sambuc anticline to the south. It is formed by Early Cretaceous to Paleocene series which are covered by gently tilted thin (~100 m) Miocene marine series. The Kyerié Basin is a small syncline located between the SW-verging Concors thrust anticline and the western Sainte-Victoire System, and is formed by Early Cretaceous series. The western terminations of the Keyrié syncline and Concors anticline as well as the Sainte-Victoire System are cut by the Aix-en-Provence fault [*Rousset*, 1978; *Guignard et al.*, 2005] and buried below Oligocene series of the Aix-en-Provence Basin (Figures 1a and 2).

2.2. Stratigraphic Succession and Geological Evolution of the Sainte-Victoire System Area

[12] Metamorphic and igneous rocks constitute the Hercynian basement of the Provence that crop outs in the Maures and Tanneron Massifs (Figure 1a). In the study area, basement rocks are reached in the Jouques exploration well (Figures 2 and 3). Basement rocks are unconformably overlain by Late Carboniferous to Permian volcanoclastic series, deposited during the rifting of Gondwana [*Delfaud et al.*, 1989]. In the western side of the Maures Massifs, thickness of these strata reaches more than 1000 m [*Cassini et al.*, 2003]. Although there is no surface or well evidences for Paleozoic sedimentary sequences in the study area, geophysical data suggest Late Paleozoic (Permian?) sequences beneath the Concors structure and western Arc syncline [*Biberon*, 1988; *Roure and Colletta*, 1996]. The overlying Mesozoic to Quaternary sedimentary pile can be divided into five structural packages: (1) Triassic to Early Cretaceous rifting sequences, (2) Late Cretaceous to Eocene Pyrenean

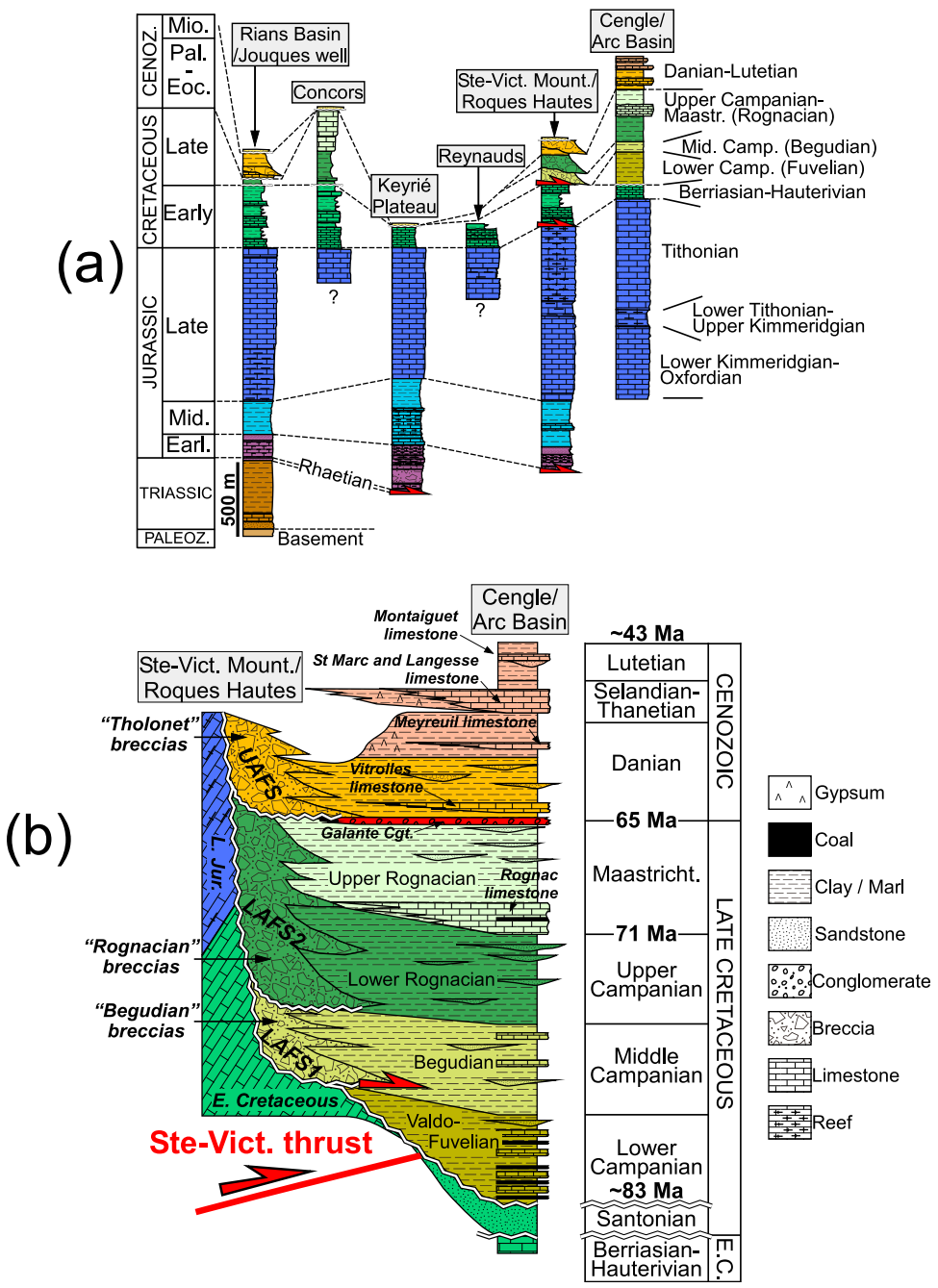

Figure 3. (a) Stratigraphic and lithotectonic sedimentary sections across the Rians Basin, Sainte-Victoire System and Arc Basin. Unconformities are shown by a snake symbol. Décollements are shown by red arrows. (b) Stratigraphic chart of the Late Cretaceous to Cenozoic series in the northwestern part of the Arc Basin. These series pinchout on deformed and overturned Mesozoic series of the western Sainte-Victoire System and correspond to syntectonic breccia deposits with growth strata pattern labeled LAFS1 (lower alluvial fan system 1), LAFS2 (lower alluvial fan system 2), and UAFS (upper alluvial fan system) in the sense of *Leleu et al.* [2005].

foreland, (3) Oligocene syn-rift deposits, (4) Miocene Alpine marine/continental sequences and (5) Quaternary continental sequences. The lithostratigraphic units are summarized in Figure 3, and described hereafter.

2.2.1. Triassic to Early Cretaceous Rifting Sequences

[13] Triassic deposits are poorly exposed in the study area. In the northern Rians syncline, the Jouques well crosses ~500 m-thick of Triassic red sandstones, shales and evaporites, which unconformably overlain the Hercynian metamorphic basement (Figure 3a). In the Sainte-Victoire System, the oldest rocks that crop out correspond to the Rhaetian rocks that can be observed along the Bimont Lake, in the core of the Sainte-Victoire Mountain structure (Figure 2). These outcrops consist of ~50 m-thick black to

green shales. Liassic series correspond to ~300 m of breccias, marine limestones and black shales in the western Sainte-Victoire System (Bimont lake). Eastward, these series are reduced to ~150 m in thickness and lack of breccia deposits (Figure 2). Middle Jurassic series correspond to ~300 m and locally more than 400 m-thick marine black shales and limestones. Late Jurassic series correspond to marine limestones, characterized by strong thickness and facies changes. In the Arc Basin and Sainte-Victoire Mountain, these series are more than 1300 m-thick and topped by massive Tithonian limestones with a reefal facies [*Tempier*, 1972] (Figures 2 and 3a). Westward, the thickness of the series decreases to ~450 m, and shows thin Tithonian limestones with basinal facies, peculiarly in the Bimont Lake (Figure 2) [*Tempier*, 1972]. Early Cretaceous series correspond to massive Berriasian marine limestones and Valanginian yellow marine limestones and shales widely exposed on the southern flank of Sainte-Victoire Mountain, Reynauds unit, Kyerié syncline, Concors and northern Rians Basin (Figure 2). Barremian to Aptian series are only exposed in the southwestern Etoile thrust and consist of marine limestones and shales (Figure 2).

[14] Since Albian and until the beginning of the Late Cretaceous, the southeastern Provence basin was uplifted and exposed above the sea level [*Masse*, 1976]. This uplift episode, named the "*Durance uplift*," separated the Alpine Basin from the Mediterranean Basin and connected the French Massif Central to the west, with the Maures Massif to the east (Figure 1a). The "*Durance uplift*" occurred during sinistral transtension of the Iberian block along the North-Pyrenean Fault associated with the opening of the central Atlantic Ocean [e.g., *Schettino and Turco*, 2011]. It is considered to be controlled either by kilometric wide crustal bend or by a local extensional regime with horsts and graben systems [*Masse and Philip*, 1976; *Guyonnet-Benaize et al.*, 2010]. Erosion of the uplifted zone was effective during the Late Cretaceous, mostly during the Cenomanian. Bauxites developed on the emerged zone (Regagnas Mountain, eastern Sainte-Victoire, Concors and Rians Basin) and were covered by foreland Santonian-Campanian sediments in the study area (Figure 2).

2.2.2. Late Cretaceous to Eocene Pyrenean Foreland and Syntectonic Sequences

[15] In the Arc Basin, subsidence and foreland deposition started in the uppermost Santonian in a marine environment and evolved into a continental environment from the lower Campanian to Eocene. In the Rians Basin, foreland sequences did not start until the upper Campanian (Figures 2 and 3a). The basal Santonian series of the Arc Basin correspond to marine sandstones only exposed in Regagnas Mountain (Figure 2). Santonian series are truncated by an erosional unconformity at the base of the continental series of the Arc Basin. The stratigraphy of the continental Late Cretaceous sequence is well known owing to the presence of exceptional dinosaur eggshells and bones together with magnetostratigraphic and biostratigraphic studies [*Westphal and Durand*, 1990; *Garcia and Vianey-Liaud*, 2001; *Cojan et al.*, 2003]. From bottom to top, the Late Cretaceous continental succession comprises: lower Campanian coal lacustrine and palustrine limestones (formerly known as "*Valdonian-Fuvelian*" local stages), middle Campanian lacustrine and fluvial deposits (formerly known as "*Begudian*" local stage); upper Campanian red fluvial siltstones with interbedded thick amalgamated sandstone beds (formerly known as "*lower Rognacian*" local stage), Maastrichtian basal lacustrine limestones and red fluvial siltstones with minor interbedded sandstone beds (formerly known as "*upper Rognacian*" local stage) (Figures 2 and 3b). Late Cretaceous series of the Arc Basin are conformably overlain by the "*Galante Formation*" of uppermost Maastrichtian. Cretaceous-Cenozoic boundary is located inside the "*Galante Formation*" (Figure 3b) [*Cojan*, 1993]. This formation, developed around the Cengle Plateau (Figure 2), consists of a lower pseudo-gley paleosols sequence [*Cojan*, 1989] and ~5–10 m-thick upper fluvial conglomerates made of well-rounded pebbles of basement quartzite, Mesozoic sandstone and limestone included in a red sandy matrix. The pebbles are less than 30 cm in diameter. Mesozoic carbonates could be locally derived while basement clasts are sourced from the Maures Massif in the east [*Cojan*, 1993] (Figure 1a). Cenozoic strata are mainly exposed in the Cengle Plateau, Palette and eastern Rians Basin areas (Figure 2). They correspond to lower Danian lacustrine limestones and orange floodplain siltstones (formerly known as "*Vitrollian*" local stage) and upper Danian to Lutetian siltstones and lacustrine limestones. Near Sainte-Victoire Mountain, gypsum and red clays are laterally equivalent to upper Danian and Lutetian lacustrine limestones (Figures 2 and 3b).

[16] Locally, foreland sequences of Arc and Rians Basins at the footwall of the Sainte-Victoire System mainly correspond to syntectonic breccias with centimetric to metric in diameter clasts exclusively sourced from Late Jurassic and Early Cretaceous series [*Durand and Tempier*, 1962; *Corroy et al.*, 1964; *Angelier*, 1971; *Tempier and Durand*, 1981; *Chorowicz and Ruiz*, 1984; *Guieu et al.*, 1987] (Figure 3b). These syntectonic breccias are organized in several stacked alluvial fan systems [*Leleu et al.*, 2005, 2009]. Two successive alluvial fan systems have been distinguished: the lower and upper alluvial fan systems (Figure 3b) [*Leleu et al.*, 2005]. The lower alluvial fan system is subdivided into a lower subsystem (LAFS1) of middle Campanian age and an upper subsystem (LAFS2) of upper Campanian-Maastrichtian age. LAFS1 and LAFS2 were formerly named "*Begudian breccias*" and "*Rognacian breccias*," respectively. The upper alluvial fan system (UAFS) is Danian in age, and overlies unconformably the previous sequences. It was formerly named "*Tholonet breccias.*"

2.2.3. Oligocene Syn-Rift Sequences

[17] During the Oligocene, E- to SE-trending extensional tectonic regimes related to the opening of the West European rift, followed by the opening of the Liguro-Provençal back-arc basins between Provence and Corsica-Sardinia block, led to the reactivation of NNE-trending faults such as the Aix-en-Provence fault. This extension is associated with the deposition of lower thick fluvial conglomerates and shales and upper lacustrine limestones [*Hippolyte et al.*, 1993]. In the study area, Oligocene deposits are mostly developed in the western Aix-en-Provence Basin and the southern Bouilladisse Basin (Figure 2).

2.2.4. Miocene Alpine Foreland Sequences

[18] During the Miocene, the post-rift subsidence and the flexure of the Alpine foreland caused marine transgression accompanied by strong planar erosion of the study area (wave-cut platform). Miocene marine series unconformably

overlie the previous unit. These series correspond to Tortonian conglomerates, calcarenites and limestones [*Besson*, 2005]. Tortonian strata are mostly exposed in the Bibemus Plateau and western Rians Basin (Figures 2 and 3a).

2.2.5. Quaternary Sequences

[19] Present-day landscape of the study area also results from prominent erosion during the Messinian sea level fall [*Clauzon et al.*, 2011] and Pleistocene glaciations. Pleistocene deposits consist of staggered strips of torrential spreadings and periglacial alluvial deposits greatly developed along the southern flank of Sainte-Victoire Mountain [*Jorda and Provansal*, 1992]. Recent alluvium deposits fill the incised valley and the Arc Basin along the Arc River (Figure 2).

2.3. Décollement Levels

[20] On the basis of mechanical stratigraphy, the main décollement level of the Sainte-Victoire System lies at the base of the Rhaetian series (Figure 3a) [*Biberon*, 1988]. Secondary shallower décollement levels are found in the Early Cretaceous limestones and shales, and at the base of the middle Campanian LAFS1 breccia sequences in the Roques Hautes area (Figures 2 and 3b) [*Chorowicz and Ruiz*, 1984].

3. Structure

[21] To constrain precisely the geometries of the Sainte-Victoire System and adjacent Arc and Rians Basins, we realized mapping at 1:5 000 scale using orthophotos combined with several field surveys, and preexisting 1:50 000 BRGM ("*Bureau de Recherches Géologique et Minière*") geologic maps of Aix-en-Provence [*Catzigras et al.*, 1969] and Pertuis [*Arlhac et al.*, 1970] (Figure 2). The mapping provides information on the sedimentary series described above and summarized in Figure 3a, age-location of syntectonic deposits (Figure 3b), bedding attitude measurements (more than 800 measures) and traces of the faults and thrusts. Exploratory wells and/or mine wells provide additional control on the depth of horizons and the thickness of the Late Cretaceous and Cenozoic sedimentary series through the Arc and Rians Basins (Figure 2). The following structural description of the study area can be separated into two parts regard to the geological map and the four surface cross sections which are presented here: (1) the western domain where the structures are mainly characterized by a southward vergence, and (2) the eastern domain with N-vergent structures (Figure 2). We present two cross sections in the western domain and two in the eastern domain (Figure 4). In the following, we will describe each cross section from north to south.

3.1. Western Sainte-Victoire System

3.1.1. Cross Section A

[22] The northern segment of cross section A cuts through the northwestern part of the Rians Basin (Figure 2). In this zone, the basin geometry corresponds to a gently deformed syncline of Early Cretaceous strata unconformably overlain by marine Miocene series, and Quaternary alluvial deposits of the Durance River. The northern limb of this syncline dips ~4° southward. Late Jurassic strata of the southern limb dip ~16° northeastward and culminate in the Concors thrust. The Concors structure corresponds to a thrust-bounded homoclinal section. The ~50° N-dipping Concors thrust cuts Early Cretaceous strata of the southern Ligourès anticline (Figure 4a). This fold is slightly asymmetric with a ~10° N-dipping northern backlimb and a ~13° S-dipping southern forelimb. To the south, the symmetric Keyrié syncline is transported southward above the Sainte-Victoire System.

[23] The western Sainte-Victoire System is associated with the broad widespread dissected Sainte-Victoire breakthrough fault-propagation fold (Figure 4a). Northward, the hanging wall flat exhibits 30°–35° N-dipping Late Jurassic limestones which form the northern cliff of the Vauvenargues valley (Figure 5a). Early Middle Jurassic shales form the axial topographic depression of the Vauvenargues valley. West of cross section A, periodic fluctuations in the water level of the Bimont Lake have resulted in lakeside exposures of Liassic breccias and Rhaetian shales (Figure 2). Southward, the hanging wall ramp consists in overturned Late Jurassic strata of the Costes Chaudes crest, dipping 70°–80° northward (Figures 4a and 5). The core and backlimb of the fold are intensely sheared by S-vergent thrust faults. The upper Bimont thrust dips ~40° northward and emplaces Rhaetian rocks above the Reynauds unit. The Reynauds unit corresponds to an overturned Late Jurassic-Early Cretaceous stratigraphic section, dipping 70°–80° northward. The 30° N-dipping Reynauds thrust cuts through prestructured Late Jurassic strata of the Costes Chaudes crest (Figure 5a), suggesting an out-of-sequence thrusting [*Ruiz Barragan*, 1978; *Chorowicz and Ruiz*, 1984]. The displacement generated along the Sainte-Victoire thrust was accommodated by the rotation of the forelimb and footwall imbrications of closely spaced thrusts involving middle Campanian-Danian series (Figures 4a and 5b). Located on the southern flank of the Sainte-Victoire anticline, the Roques Hautes unit includes middle Campanian to Danian syntectonic breccia deposits (Figure 6a; see also more details in Figure 7). The southern Roques Hautes structure corresponds to a S-vergent fault-bend fold that exhibits a 60° N-dipping hanging wall flat at the base of the middle Campanian breccias (Marble Ridge structural relief; Figures 5b and 7) of the LAFS1. These breccia deposits are overlain by upper Campanian-Maastrichtian red marls and limestones that progressively pass northward to breccia deposits of the LAFS2. Surface data show that breccia sequences of LAFS1 and 2 pinchout northward onto the Costes Chaudes ridge, as described by *Leleu et al.* [2009] (Figure 6a). The dip of the Roques Hautes thrust was initially probably lower and was back-tilted during the imbrication of the Harmelins folds to the south. The structural frame of the Harmelins unit consists in two "*en-echelon*" fault-propagation folds, both armed of Maastrichian limestones (Figure 2). Along cross section A, the southern fold exhibits a breakthrough style (Figure 7). The upper thrust places Maastrichtian limestones onto S-dipping to overturned Danian breccias of the UAFS. In details, the breccia layers are strongly deformed by subhorizontal S-vergent thrust and back-thrusts, and are thrust to the south onto the Cenozoic strata of the Arc Basin (Cengle Plateau) along the Sainte-Victoire thrust (Figures 6b and 7).

[24] The Arc Basin located at the footwall of the western Sainte-Victoire System corresponds to an asymmetrical syncline mainly formed by Late Cretaceous continental series. The core of the syncline is formed by subhorizontal

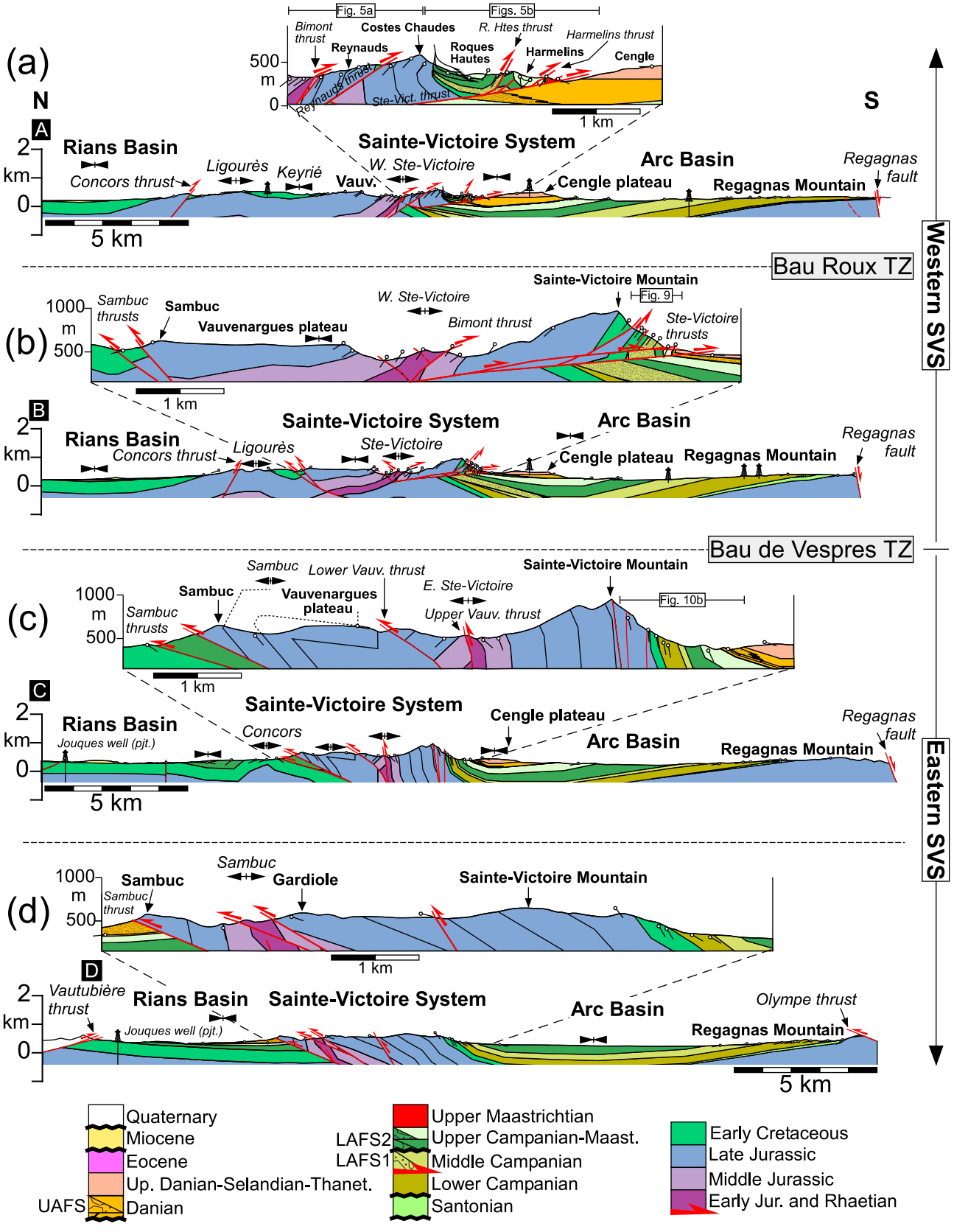

Figure 4. Surface cross sections across the western (A and B) and eastern Sainte-Victoire Systems (C and D). For location, see Figure 2. Details of the Sainte-Victoire thrust systems are also shown.

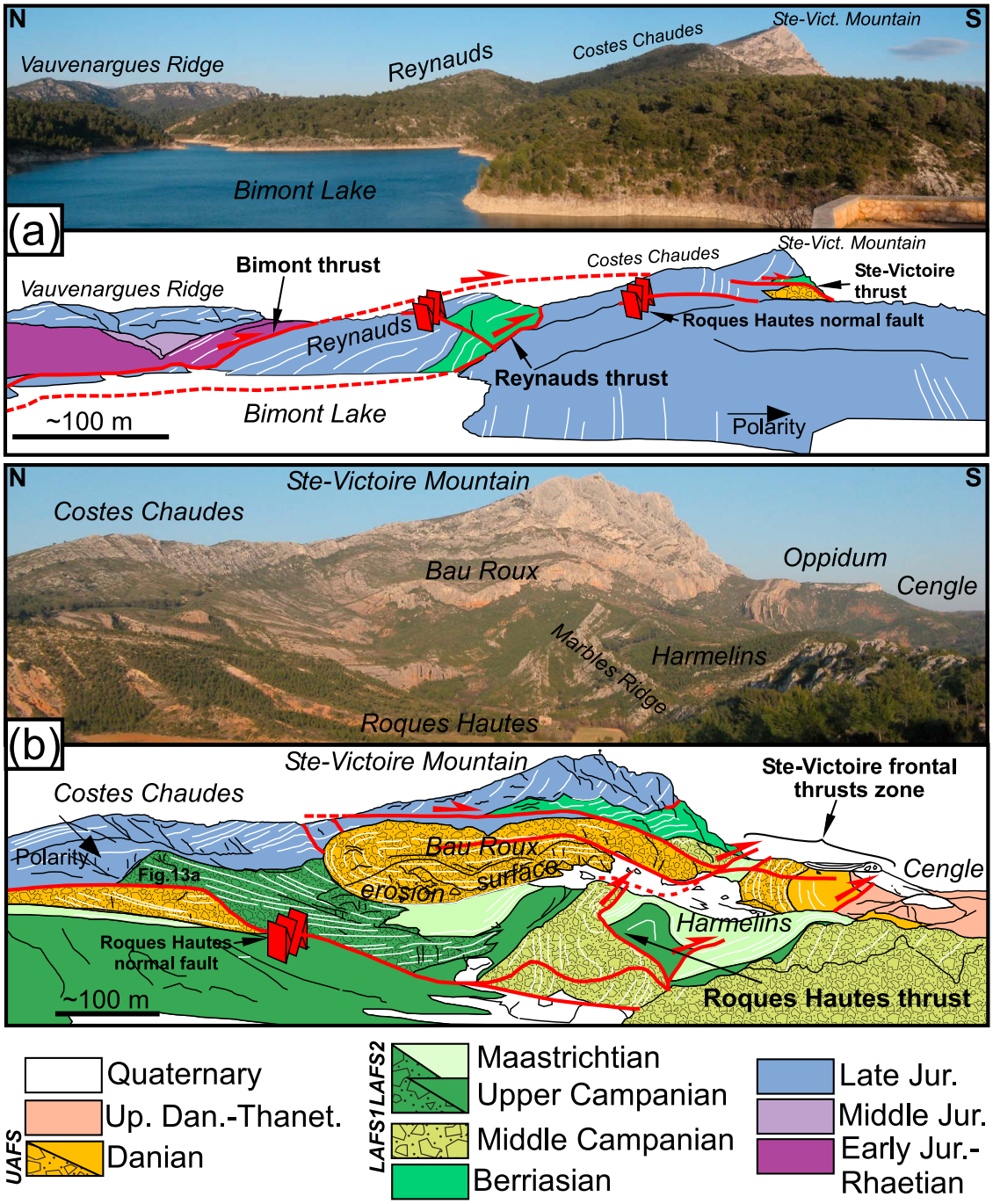

Figure 5. East-looking panoramic views of the western Sainte-Victoire System. (a) Detail of northern thrust system in the Bimont lake area (cross section A; 858 908E, 1 843 000N). (b) Detail of the Roques Hautes thrust system with Late Cretaceous syntectonic filling (858 670E, 1 842 000N). Foreground: trace of cross section A across the Costes Chaudes ridge. Background: trace of cross section B′ across Sainte-Victoire Mountain (Figure 8). Bedding traces are enhanced by white lines and faults traces by thick red lines. For location, see Figures 4a and 4b.

Cenozoic strata of the Cengle Plateau. These series are affected by minor fold and thrusts, possibly related to transfer of shortening from the Sainte-Victoire System. The southern limb exhibits 5–10° N-dipping lower Campanian series, cut by the Regagnas Mountain S-dipping normal fault. In the construction of cross section A, we assumed a similar thickness of sedimentary series on both sides of the Sainte-Victoire thrust. Using this assumption together with field and subsurface data, cross section A shows that the western Arc syncline exhibits two superimposed and opposed sedimentary wedge-shaped geometries (Late Cretaceous and Danian) (Figure 4a). The thickness of the Late Cretaceous wedge decreases northward, from ~1600 m in Regagnas Mountain to less than ~600 m in the footwall of

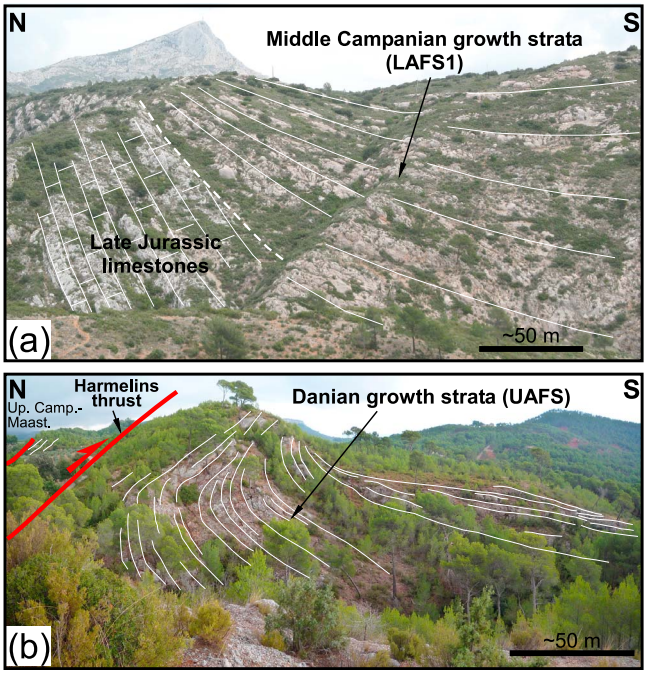

Figure 6. (a) Growth stratal pattern in middle Campanian breccia sequences (LAFS1) on the western edge of the Costes Chaudes ridge, southern flank of the Sainte-Victoire anticline (west of section A; 858 255E, 1 842 295N). (b) Growth stratal pattern in Danian breccia sequences (UAFS) at the front of the Harmelins thrust (west of section A; 858 319E, 1 841 044N). Bedding traces are enhanced by thin white lines and faults traces by thick red lines.

the Sainte-Victoire thrust. In contrast, the thickness of Danian wedge decreases southward, from 350 m to the north to 200 m to the south.

3.1.2. Cross Section B

[25] Cross section B (Figure 4b) shows a similar structural geometry of the Rians syncline, Concors thrust and Ligourès anticline as in cross section A. However, the structure of the Sainte-Victoire System is characterized by a bi-vergence of the thrust systems [*Chorowicz and Ruiz*, 1984; *Biberon*, 1988; *Roure and Colletta*, 1996]. The Kyerié syncline forms the footwall of the N-vergent Sambuc thrust. Near the eastern termination of the Concors anticline, the Sambuc thrust is linked with at least two branches. The southern Sambuc thrust dips ~50° to the south and places 15° N-dipping Late Jurassic strata above 5°–10° N-dipping Early Cretaceous strata. The slip on the Sambuc thrust significantly increases eastward (Figures 2 and 4b), and Late Jurassic beds of the hanging progressively become overturned (Sambuc Ridge). Southward, gently deformed N-dipping Jurassic strata form the hanging wall flat of the Sainte-Victoire fault-propagation fold. Southward, massive upper Jurassic reef limestones form the overturned forelimb of the Sainte-Victoire anticline (Figure 4b) [*Tempier*, 1972]. Jurassic series of the hanging wall flat dip 18° northward along the Vauvenargues cliff and more steeply (~40°) in the valley. As for cross section A, the core and overturned forelimb of the anticline were intensely folded and sheared by breakthrough branches of the Sainte-Victoire Mountain thrust system. The core of the anticline is cut by the upper Bimont thrust. This thrust dips ~45°–50° northward and emplaces Liassic rocks over overturned Middle Jurassic strata. Southward, the Sainte-Victoire thrust splits into at least two branches. The upper branch cuts the 60°–70° N-dipping

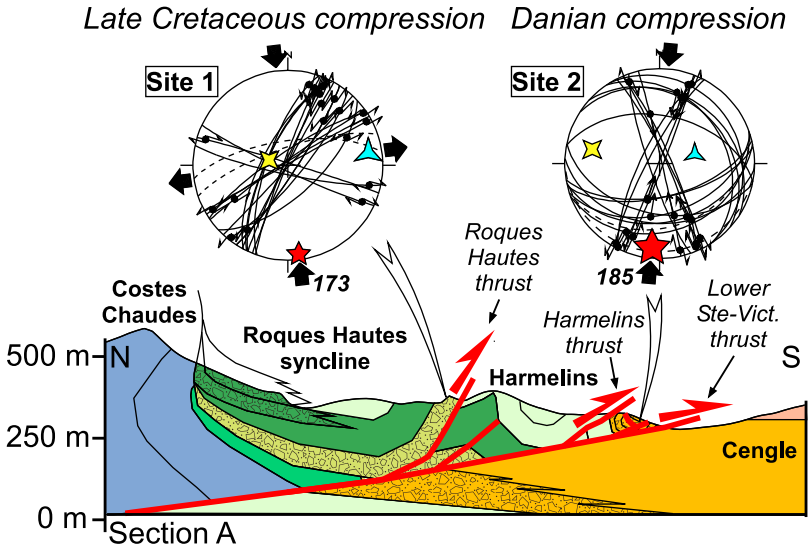

Figure 7. Polyphased faulting in the growth strata deposits of the Roques Hautes area and detail of cross section A. Site 1 is located in the middle Campanian breccias (LAFS1). N-dipping breccia layers are cut by post-tilt strike-slip faults indicating NNW-trending compression. Site 2 is located in the Danian breccias (UAFS). S-dipping breccia layers are cut by strike-slip and reverse faults indicating NNE-trending compression. Fault data are projected in an equal area stereogram, lower hemisphere. Principal stress axes ($\sigma 1$, $\sigma 2$, and $\sigma 3$) are symbolized by red five-branch, yellow four-branch, and blue three-branch stars, respectively. Trend of $\sigma 1$ is shown. Dashed line corresponds to the projection of bedding dip in the stereogram.

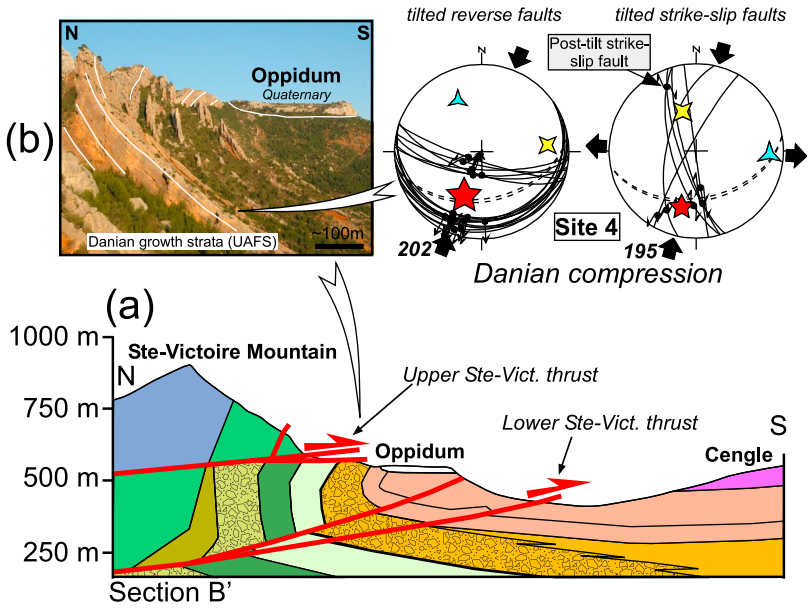

Figure 8. Syn-Danian growth strata compression at the front of Sainte-Victoire Mountain. (a) Detail of cross section B′. For location, see Figure 2. (b) Site 4 shows deformed reverse and strike-slip faults indicating similar NNE-trending compression synchronous to the sedimentation of the Danian UAFS. Note that one strike-slip fault is post-tilting. Fault data are projected in an equal area stereogram, lower hemisphere. Principal stress axes ($\sigma 1$, $\sigma 2$, and $\sigma 3$) are symbolized by red five-branch, yellow four-branch, and blue three-branch stars, respectively. Trend of $\sigma 1$ is shown. Dashed line corresponds to the projection of bedding dip in the stereogram.

overturned forelimb of the Sainte-Victoire anticline, and emplaces middle Campanian breccias (LAFS1) over strongly sheared Maastrichtian series (Figure 4b). More southward, the lower branch emplaces intensively sheared syntectonic Danian deposits (UAFS) over Selandian evaporites and clays (Figure 4b; see also cross section B′ in Figure 8a). Displacement above these thrusts significantly decreases in the transport direction. Currently, the overturned forelimb of the Sainte-Victoire anticline shows large-scale E-trending subvertical faults. These structures correspond to N-vergent thrusts that have been rotated to an overturned position during the emplacement of the Sainte-Victoire anticline (Figure 9). Initially, these thrusts propagated northward through the central Sainte-Victoire backlimb, probably as a result of flexural slip or frictional resistance associated with fault slip [*Mitra*, 2002].

[26] As for cross section A, the Arc Basin corresponds to an asymmetrical syncline mainly formed by the Late Cretaceous and cored by Cenozoic series of the Cengle Plateau (Figure 4b). In contrast with cross section A, the syncline is characterized by a steep to overturned northern limb intensely deformed by the S-vergent Sainte-Victoire thrust. The southern limb of the syncline dips ~10° northward and shows minor faulting and internal folding within Campanian series. Southward, Late Jurassic limestones, unconformably overlain by Santonian marine limestones and grainstones, form the crest of Regagnas Mountain. More southward, these strata are cut by S-dipping normal faults of Regagnas Mountain (Figure 4b). Assuming similar thickness of sedimentary series on both sides of the Sainte-Victoire thrust, we show that the foreland sedimentary package of the Arc Basin exhibits a wedge-shaped geometry thinning northward. Based on field evidence, cross section B shows a thickness decrease of the Late Cretaceous wedge, from ~1600 m in Regagnas Mountain to less than ~450 m toward the Sainte-Victoire thrust. Besides, the overlying Danian wedge thins northward, from 140 m to the south, to less than 50 m to the north.

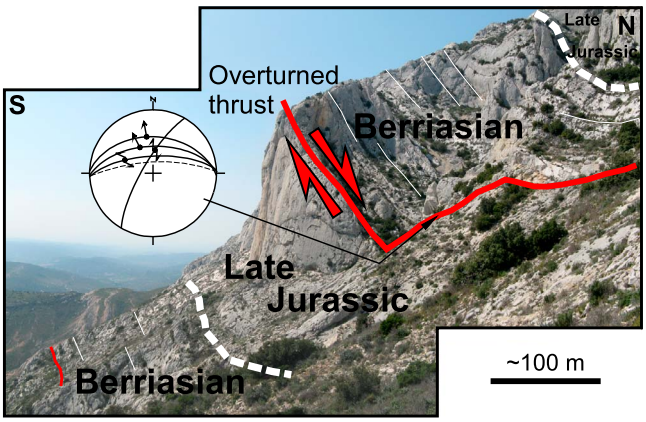

Figure 9. Overturned N-vergent thrust in the southern flank of Sainte-Victoire Mountain, between cross sections B and B′ (For location, see Figure 4b; 863 949E, 1 841 726N). Currently, kinematic indicators measured along the overturned thrust trace show normal faulting. Bedding traces are enhanced by white lines. Fault data are projected in an equal area stereogram, lower hemisphere. Dashed line corresponds to the projection of hanging wall bedding dip in the stereogram.

3.2. Eastern Sainte-Victoire System

3.2.1. Cross Section C

[27] Along cross section C (Figure 4c), the Rians Basin is composed of sub-horizontal Early Cretaceous strata unconformably overlain by Miocene marine deposits. Southward, the cross section cuts the eastern termination of the Concors anticline lying between a northern narrow syncline filled by Maastrichtian continental sequences and the Sambuc thrust in the south. Here, the Concors anticline is asymmetric. Its tip line plunges southeastward below the Sainte-Victoire System. The northern limb dips ~22° northward and more steeply (~40°) to the north while the southern limb dips 35° southward. Southward, cross section C crosses the Sambuc and the eastern Sainte-Victoire imbricated thrust anticlines. The northern Sambuc structure corresponds to a fault-propagation fold characterized by an overturned forelimb, dipping 50° southward and a 9° S-dipping backlimb. The geometry of the backlimb has been complicated by S- and N-vergent small-scale disharmonic folds within Late Jurassic series. South of the Sambuc unit, the Sainte-Victoire structure is an upper breakthrough fault-propagation fold, emplaced along the lower Vauvenargues thrust (Figure 4c). The hanging wall ramp consists in Middle to Late Jurassic strata dipping 40°–45° northward. The core of the Sainte-Victoire anticline is formed by strongly sheared Liassic sequences above the upper Vauvenargues thrust (Figure 4c). Jurassic beds of the southern hanging wall flat are vertical and form the highest crest of Sainte-Victoire Mountain (1011 masl). This crest is affected by NE-trending subvertical faults, that cut Late Jurassic and Early Cretaceous strata (Figures 4c and 10b).

[28] Cross section C shows that the Arc Basin was transported northward on the hanging wall of the Sainte-Victoire System (Figures 4c and 10b). The geometry of the Arc Basin corresponds to an asymmetrical syncline. The southern limb forms a long homocline dipping ~10° northward, where the exposed Late Cretaceous continental sequences reach 1.2 km-thick to the south. Southward, the steeply dipping Regagnas Mountain normal fault affects Late Jurassic and Santonian series. Located in the hanging wall of the lower Vauvenargues thrust, the northern limb of the Arc syncline is steeply dipping (80–85°) southward and exposes Late Cretaceous continental sequences of ~700 m in thickness (Figures 4c and 10b). Santonian marine series pinchout toward the north while Early Cretaceous series pinchout toward the south. The core of the syncline is formed by uniformly thick Paleocene sequences of the Cengle Plateau.

3.2.2. Cross Section D

[29] Along cross section D (Figure 4d), the eastern Rians Basin lies between the Vautubière and Sambuc thrusts (Figure 2). The S-vergent Vautubière thrust places Jurassic rocks onto Early Cretaceous and foreland series of the Rians Basin. Both seismic reflection data presented by *Biberon* [1988] and field data show that the structure of the eastern Rians Basin consists of S-dipping (~3°) thick Jurassic to Early Cretaceous limestones. An upper Campanian-Danian foreland continental package unconformably overlies Jurassic to Early Cretaceous rocks and thins northward. The maximum thickness of these series is found near the Sambuc thrust, where they gently dip to the north. The Sambuc anticline corresponds to a main breakthrough fault-propagation fold that is developed above the Sambuc thrust. This thrust dips 22° southward and cuts Danian breccia strata of the Rians Basin (Figure 4d). The core of the fold is formed by Liassic shales. The hanging wall ramp consists in overturned Middle and Late Jurassic strata dipping 70°–80° southward. Beds in the southern backlimb of the anticline are ~55° to 30° S-dipping from the north to the south. The Sambuc anticline backlimb pattern corresponds to an imbricate zone of three S-dipping thrust faults, duplicating Jurassic series.

[30] As shown in cross section C, the Arc Basin is transported on the hanging wall of the Sainte-Victoire System (Figures 4c and 4d). Here, the geometry of the Arc syncline is almost symmetrical. The northern limb dips 16° southward and the southern limb dips ~12° northward (Figures 4d and 10b). Southward, Late Jurassic and Santonian series are cut by the north vergent Olympe thrust (Figure 2). Late Cretaceous lower red clays are exposed at the axis of the syncline. The exposed Late Cretaceous continental sequences are ~700 m-thick and no significant thickness variations have been recognized. As for cross section C, Santonian marine series pinchout toward the north while Early Cretaceous series pinchout toward the south (Figures 4c and 4d).

4. Syntectonic Sedimentation

[31] Growth strata provide a record of the timing of deformation in foreland basins [e.g., *Suppe et al.*, 1992; *Meigs and Burbank*, 1997]. Growth strata patterns are recognized within the Late Cretaceous-Danian alluvial fan systems on both flanks of the Sainte-Victoire System [e.g., *Leleu et al.*, 2005, 2009, and references therein]. However, the syntectonic sedimentation shows that complex spatial and temporal growth strata arrays may be related to several thrust pulses and along-strike deformation partitioning through Late Cretaceous to Cenozoic times. In the following, we describe growth strata on both flanks of the Sainte-Victoire System.

4.1. Southern Flank of the Sainte-Victoire System

[32] Syntectonic deposits develop in the Roques Hautes and Sainte-Victoire Mountain thrust systems (Figure 2). As shown in cross section A (Figure 4a), middle Campanian to Maastrichtian coarse breccia deposits (attributed to LAFS1 and LAFS2) of the inner Roques Hautes syncline exhibit progressive stratal dip increase (from 0° to 85°S) and thinning with intraformational unconformities toward the Costes Chaudes ridge (Figures 5b and 6a) [*Leleu et al.*, 2009]. Preserved Danian growth strata deposits of the UAFS develop laterally to cross section A in the eastern Bau Roux and western Zola areas [*Leleu et al.*, 2009] (Figure 2). The progressive backlimb rotation of the western Sainte-Victoire anticline would be recorded from middle Campanian-Maastrichtian until Danian times. However, the panoramic view of Figure 5b shows that the eastern tip of the Roques Hautes thrust is sealed by sub-horizontal series of the UAFS. This suggests that the Roques Hautes thrust was deactivated since Danian. Southward, the growth of the southern Harmelins anticline was recorded by the UAFS (Figure 6b). Although deposits of the UAFS are intensively deformed, growth strata geometry can be clearly recognized in the

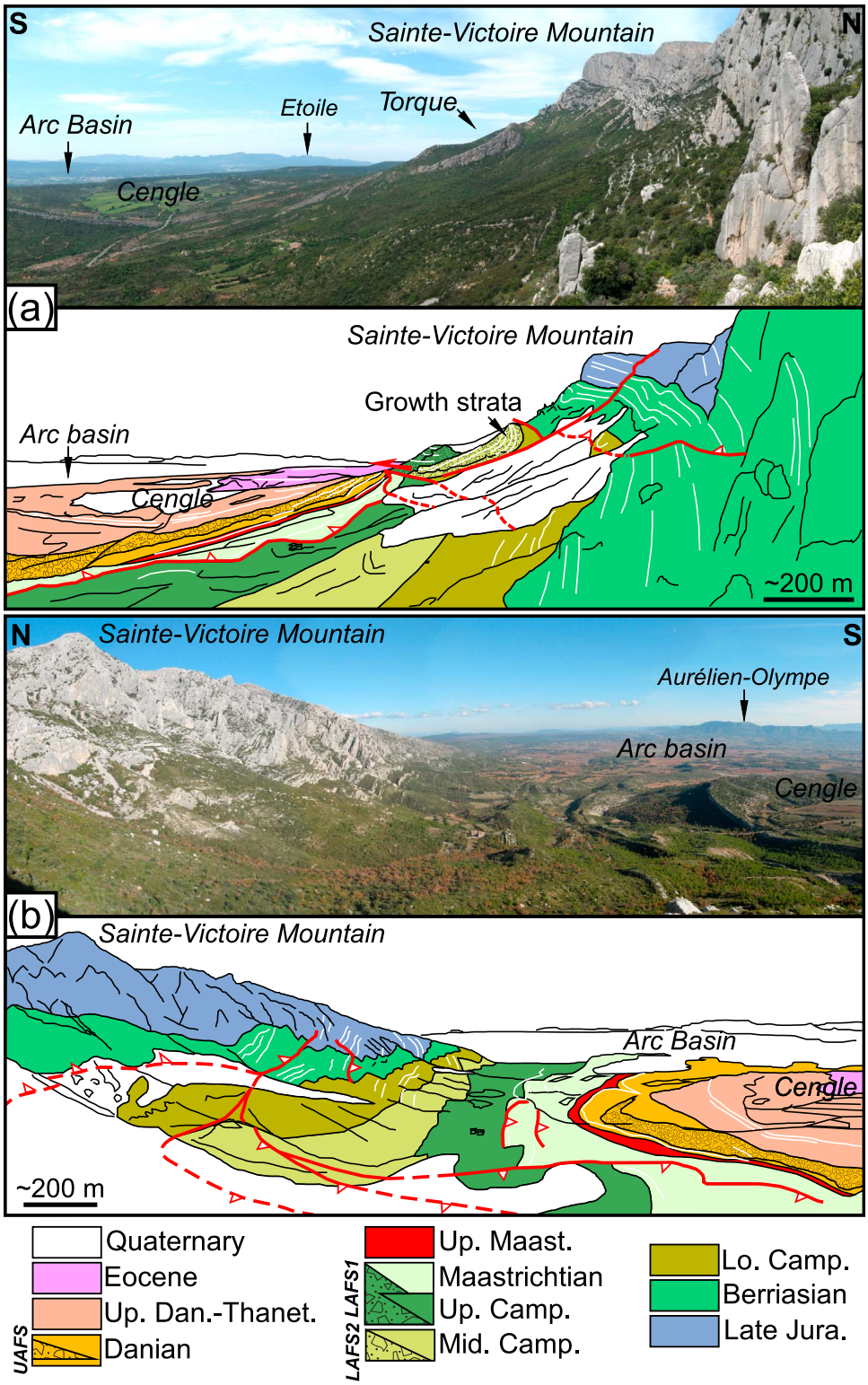

Figure 10. Panoramic views of the transition between the western and eastern Sainte-Victoire Systems. (a) Bau de Vespres transverse structure and progressive back thrusting of the southern flank of Sainte-Victoire Mountain (view looking to the west, 865 963E, 1 841 866N). Note growth strata in LAFS1 of the Torque syncline. (b) Southern part of cross sections C and D across the eastern Sainte-Victoire System (view looking to the east, 867 376E, 1 842 212N). Bedding traces are enhanced by white lines. For location, see Figures 4c and 4d.

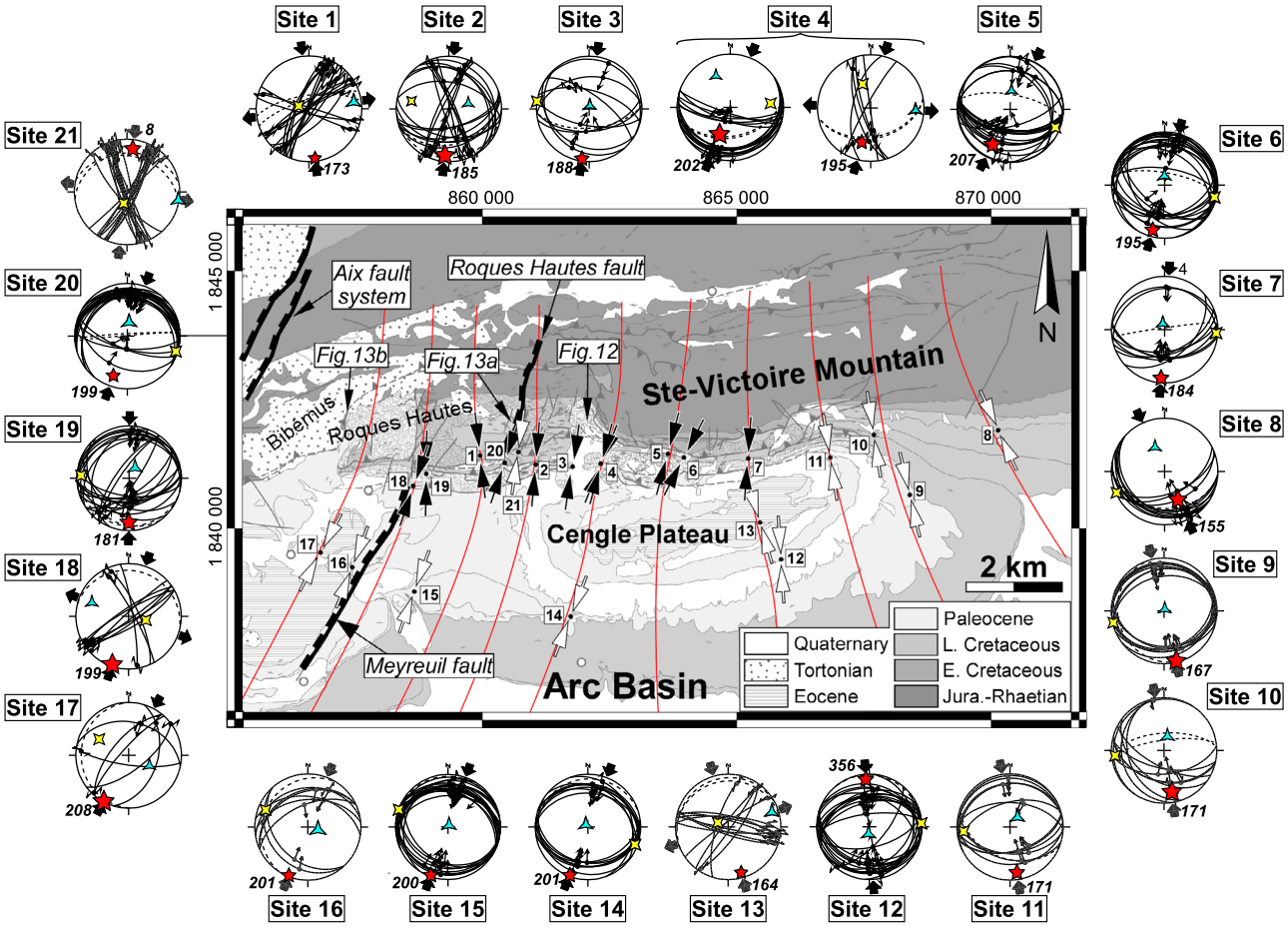

Figure 11. Pyrenean directions of compression south of the Sainte-Victoire System. Site numbers are shown by white squares. Black arrows: Fault site in growth strata. White arrows: Inferred Late Cretaceous-Eocene compression. Fault data and principal stress axes are also shown. Principal stress axes (σ1, σ2, and σ3) are symbolized by red five-branch, yellow four-branch, and blue three-branch stars, respectively. Trend of σ1 is shown. Data are projected in an equal area stereogram, lower hemisphere (see Table 1). Dashed line corresponds to the projection of bedding dip in the stereogram. Site 1 has been measured within middle Campanian growth strata of the LAFS1. Sites 2, 3, 4, 5, 6, 7, 18, 19, 20 have been measured within Danian growth strata of the UAFS. Other sites are measured in lower Campanian to Lutetian sedimentary series. The mean direction of compression is N-trending with inner and outer fan-shaped deviations (red lines). Major Oligocene normal faults (Aix, Meyreuil and Roques Hautes faults) and location of Figure 12 and Figures 13a and 13b are also shown.

UAFS, indicating thrusting activity at the leading edge of the Sainte-Victoire System at least since the Danian.

[33] In cross sections B, similar observations are made along the southern flank of Sainte-Victoire Mountain. For example, the eastern Torque syncline exhibits breccia layers of LAFS1 and LAFS2 intercalated with Maastrichtian sandstones and red clays (Figure 10a). The dip of these strata increases progressively northward with decreasing thicknesses, attesting for growth stratal pattern. LAFS1 and LAFS2 growth strata have thus recorded the growth of the Torque syncline and the activity of the upper Sainte-Victoire thrust during middle Campanian to Maastrichtian times. As shown on panoramic views of Figures 5b and 10a, and cross sections B (Figure 4b), the activity of the lower Sainte-Victoire thrust was recorded by growth strata of the UAFS. Although UAFS growth strata overlie Maastrichtian series to the west, they are progressively intercalated within Danian series to the east (eastern edge of the Cengle Plateau, cross section C; Figures 2 and 4c). More eastward, the deformation timing cannot be clearly defined because most of the Late Cretaceous and Cenozoic foreland series were eroded. To sum up, middle Campanian (LAFS) and Danian (UAFS) growth strata recorded the growth of the western S-vergent Sainte-Victoire System in the Arc Basin.

4.2. Northern Flank of the Sainte-Victoire System

[34] In the eastern Rians syncline, only the LAFS2 and the UAFS were deposited, and no record of the LAFS1 is found (Figure 2) [e.g., *Leleu et al.*, 2009]. LAFS2 strata unconformably overlie Hauterivian marine deposits near the southern thrust front of Vautubière Mountain (Figure 2). Breccia layers exhibit growth strata geometry, suggesting that the growth of the Vautubière anticline was active during upper Campanian-Maastrichtian period. The northern flank

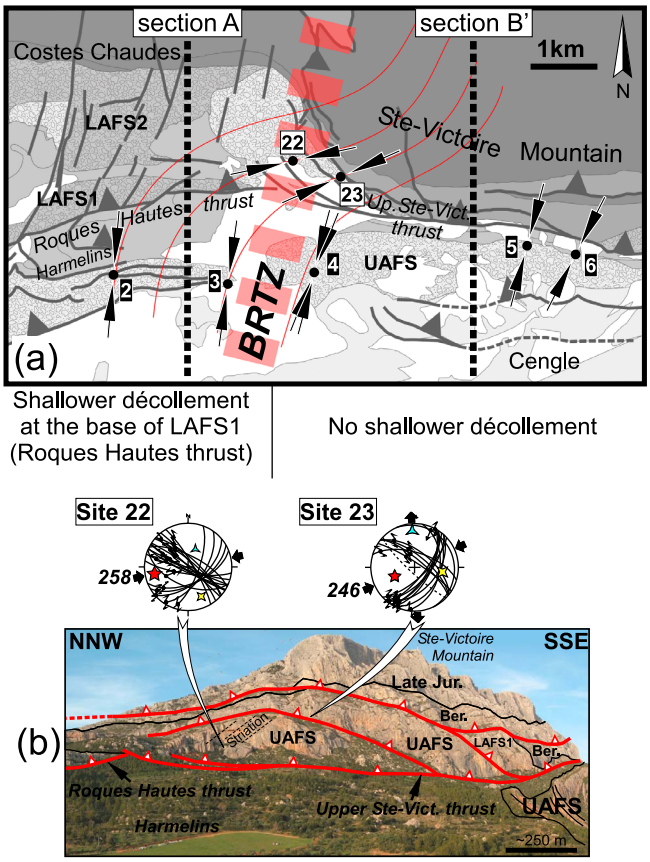

Figure 12. (a) Geologic map of the Bau Roux transverse zone (BRTZ, dashed thick red area) with location of additional sites 22 and 23 measured within Danian breccias of the UAFS (white framed numbers; see Table 1). (b) Panoramic view, looking to the northeast, of the Bau Roux transverse zone. Location of sites 22 and 23 is also shown. Fault data are projected in an equal area stereogram, lower hemisphere. Trend of $\sigma 1$ is shown. For legend, see Figure 11. The local ENE-trending directions of compression at the western edge of Sainte-Victoire Mountain are compatible with stress deviations (red lines) occurring between the Sainte-Victoire Mountain and Roques Hautes thrust systems.

of the Concors anticline shows no breccia deposits [*Cojan*, 1989]. In the eastern Rians Basin, Danian breccias of the UAFS are deposited unconformably on the Maastrichtian series. North of the Sambuc thrust, Danian breccias of the UAFS are intercalated within lacustrine package (Figure 4d) [*Leleu et al.*, 2009]. The breccia layers pinchout toward the north. Although growth strata geometry is not clearly recognized within Danian breccia deposits of the UAFS, we propose that these series recorded the growth of the eastern N-vergent Sainte-Victoire System in the Rians Basin, as suggested by *Angelier* [1971].

5. Pyrenean Compressional Stress Regime as Revealed by Fault Slip Analysis and Post-Pyrenean Deformations in the Sainte-Victoire System

[35] Fault slip analysis in thrust belts permits to relate the formation of large scale structures to paleostress directions, and to determine the chronology of successive deformational events in case of complex structures [e.g., *Angelier*, 1990; *Hippolyte et al.*, 2012]. Fault slip analysis presented in this study was carried out to constrain the structural evolution of the Sainte-Victoire System. In the frame of the polyphase tectonic evolution of Provence, many models were suggested to explain this outstanding structure (see chapter 1 for references). Therefore, a detailed fault slip analysis is necessary to unravel the possible complex origin of the Sainte-Victoire System and to determine the direction to be considered for correctly restoring cross sections.

[36] The fault slip analysis is based on the assumption that slickenside lineations on a fault plane indicate both the direction and sense of maximum resolved shear stress on fault plane. If the stress state is known, one can derive the shear stress orientation (slip vector) on any fault plane. By measuring the slip directions of fault planes of various orientations, one can solve the inverse problem and determine an average stress tensor [e.g., *Carey and Brunier*, 1974; *Angelier et al.*, 1982]. Variations in stress regimes through time can be stratigraphically dated by reconstructing paleostresses at different stratigraphic levels. Furthermore, the fault slip analysis in growth strata deposits provides a direct dating of the paleostresses and allows to relate large scale structures to this dated stress regime. To achieve that, fault slips predating and postdating the synsedimentary deformation have to be recognized [*Hippolyte et al.*, 1992]. Although some paleostress studies have already been done in the Sainte-Victoire System area and Arc Basin [*Gaviglio*, 1985; *Gaviglio and Gonzales*, 1987; *Lacombe et al.*, 1992; *Andreani et al.*, 2010; *Hippolyte et al.*, 2012], this method was not applied to the kinematic interpretation of specific large scale structures and in particular to growth strata as in this study. *Lacombe et al.* [1992] identified the Pyrenean N-trending compression by a fault kinematic study in the western Sainte-Victoire Mountain. They also identified the Oligocene E-trending extension and the ENE- to NE-trending Alpine compression. The best way to characterize the Pyrenean deformation pattern and to support the N-S trend as the correct direction for restoring the cross sections, is to analyze brittle tectonics in the coeval growth strata deposits. In the study area, we measured faults with a clear sense of movement on various scale faults and we calculated paleostress in 24 sites to infer the kinematics of large scale structures (see location of measurement sites in Figures 11, 12, and 13, and data in Table 1). This analysis is composed of 13 sites in the growth strata developed in the western S-vergent Sainte-Victoire System which allows to accurately date the reconstructed state of stress, and 11 sites in lower Campanian to Lutetian sedimentary series (Table 1).

5.1. Pyrenean Compressional Stress Recorded by Growth Strata

[37] We measured strike-slip faults in the middle Campanian breccias of the LAFS1 in the southern flank of the Roques Hautes syncline (site 1; Figures 7 and 11). The breccia layers dip 72° toward the north. Paleostress computation shows a NNW-trending compression (Figures 7 and 11). We propose that this compression, perpendicular to the trend of the bedding, is responsible for the folding. Therefore, this NNW-trending compression would be active in the Roques Hautes

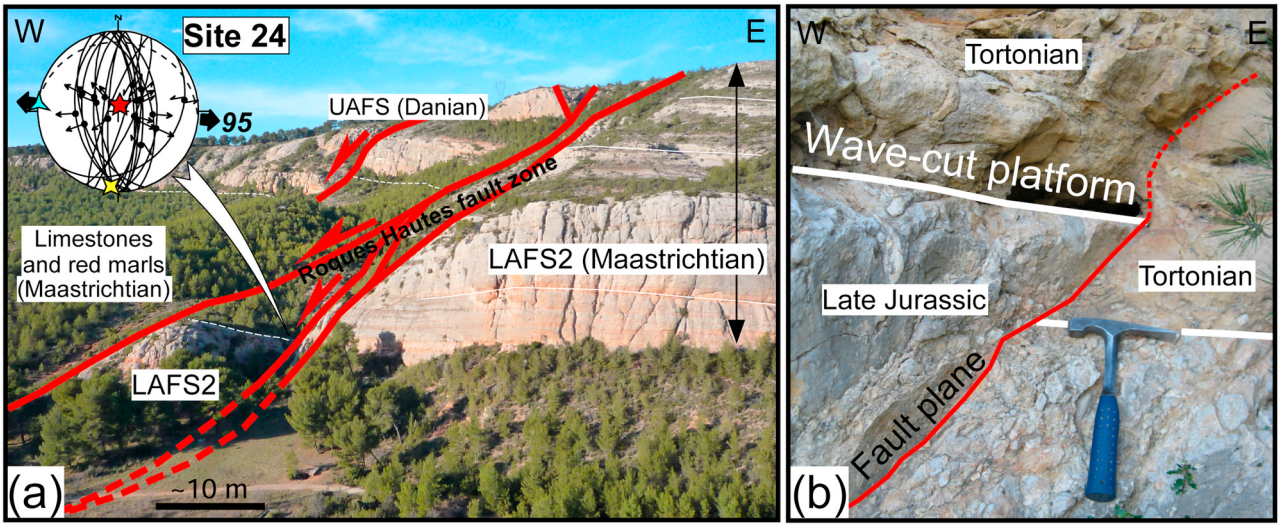

Figure 13. Two field examples of post-Pyrenean deformation in the western Sainte-Victoire System. (a) Roques Hautes fault zone in the western Sainte-Victoire System affecting deformed LAFS2 and UAFS growth strata (860 173E, 1 841 947N). This fault zone is associated with an E-trending extension, post-dating the Pyrenean compression. Fault data (Table 1) are projected in an equal area stereogram, lower hemisphere. Trend of $\sigma 1$ is shown. For legend, see Figure 11. Bedding traces are enhanced by thin white lines. See locations in Figure 5b and Figure 11. (b) Small scale strike-slip fault affecting basal surface (wave-cut platform) of Tortonian marine sequences (856 592E; 1 842 211N). For location, see Figure 11.

Table 1. Paleostress Tensors Computed From Fault Slips and Measured at the Sites of Figures 11, 12, and 13[a]

Site	Longitude (m)	Latitude (m)	Elevation (masl)	Age/Lithology	Nb of Faults	$\sigma 1$		$\sigma 2$		$\sigma 3$		Φ	ANG	RUP	Stress Regime
						Trend	Plunge	Trend	Plunge	Trend	Plunge				
1	859372	1841337	346	Middle Campanian/ Breccias (LAFS1)	20	173	6	285	73	81	15	0.69	14	30	strike-slip
2	860463	1841177	291	Danian/Breccias (UAFS)	21	185	12	282	28	75	59	0.11	13	38	strike-slip reverse
3	861223	1841120	297	Danian/Breccias (UAFS)	9	188	5	278	0	10	85	0.51	12	36	compressional
4	861910	1841321	338	Danian/Breccias (UAFS)	17	202	45	284	25	335	35	0.08	8	31	compressional
4	-	-	-	-	6	195	34	341	51	93	17	0.54	22	55	strike-slip
5	863357	1841315	506	Danian/Breccias (UAFS)	24	207	27	112	10	4	61	0.34	10	40	reverse
6	863429	1841334	515	Danian/Breccias (UAFS)	25	195	13	104	4	358	76	0.45	8	32	reverse
7	864637	1841219	517	Danian/Breccias (UAFS)	9	184	10	94	3	344	80	0.41	4	13	compressional
8	870216	1842009	396	Early Campanian/ Limestones	11	155	41	246	2	339	49	0.24	5	43	compressional
9	868358	1840388	359	Danian/Limestones	16	167	2	257	2	24	87	0.2	6	41	compressional
10	867261	1841789	424	Maastrichian/Limestones	9	171	21	264	8	14	68	0.32	9	18	compressional
11	866660	1841375	438	Selandian-Thanetian/ Limestones	12	171	13	265	13	37	71	0.55	11	28	compressional
12	865458	1839150	445	Selandian-Thanetian/ Limestones	26	356	11	86	2	187	79	0.45	9	28	compressional
13	865335	1839936	483	Lutetian/Limestones	13	164	11	292	73	71	13	0.81	6	27	strike-slip
14	861269	1837937	281	Danian/Limestones	15	201	2	111	5	316	85	0.37	7	29	compressional
15	857936	1838421	198	Danian/Limestones	25	200	3	290	1	30	87	0.46	10	37	compressional
16	856808	1839020	190	Selandian-Thanetian/ Limestones	8	201	2	292	16	103	74	0.71	7	24	compressional
17	865172	1839351	190	Lutetian/Limestones	6	208	1	299	36	117	54	0.08	19	56	strike-slip reverse
18	858135	1840684	221	Danian/Breccias (UAFS)	10	199	4	101	63	290	27	0.2	6	17	strike-slip
19	858283	1841041	260	Danian/Breccias (UAFS)	22	181	17	273	9	30	71	0.25	9	27	compressional
20	859859	1841145	258	Danian/Breccias (UAFS)	22	199	22	108	4	7	68	0.65	7	16	compressional
21	860015	1841395	269	Maastrichian/Sandstones	22	8	18	196	71	98	2	0.32	8	28	strike-slip
22	861914	1841921	645	Danian/Breccias (UAFS)	19	258	22	156	27	22	54	0.22	13	35	strike-slip
23	861732	1841943	544	Danian/Breccias (UAFS)	15	246	49	100	36	356	17	0.53	12	27	strike-slip
24	860186	1841912	312	Maastrichtian/ Breccias (LAFS2)	18	16	83	185	7	275	1	0.49	15	41	extensional

[a]Coordinate system is Lambert 2, Paris system (meters). $\sigma 1$, $\sigma 2$, $\sigma 3$: maximum, intermediary and minimum principal stress axis, respectively. $\Phi = (\sigma 2 - \sigma 3)/(\sigma 1 - \sigma 3)$. ANG = average angle between computed shear stress and observed slickenside lineation (in degrees). RUP = quality estimator ($0 \leq RUP \leq 200$) taking into account the relative magnitude of the shear stress on fault planes (see *Angelier* [1990] for more details).

syncline, at least during the middle Campanian-Maastrichtian times.

[38] We also measured faults in the Danian growth strata of the UAFS that develop in the Sainte-Victoire and Roques Hautes thrust systems (sites 2, 3, 4, 5, 6, 7, 18, 19 and 20; Figure 11). For instance at site 4, in S-dipping breccia layers at the front of Sainte-Victoire Mountain, we measured normal and steeply dipping reverse faults, and strike-slip faults (Figure 8). Backtilting of the normal and steeply dipping reverse faults shows a system of conjugate reverse faults consistent with a horizontal NNE-trending compression, assuming that compressive $\sigma 1$ was horizontal when bedding planes were horizontal. Strike-slip faults show sub-horizontal to bedding parallel striations. These faults are also consistent with the same NNE direction of compression. The post-tilt strike-slip fault of site 4 (Figure 4) shows that deformation also occurred after the tilting of the growth strata. Therefore, we can conclude that a strike-slip reverse deformation corresponding to the NNE compression occurred during this tilting.

[39] To sum up, fault slip analysis in growth strata of the UAFS shows: (1) pre-tilt compression (2 stress axes parallel to the bedding planes) at sites 4 and 19, (2) syn-tilt compression ($\sigma 1$ less tilted than bedding planes) at sites 2, 4, 5 and 20, and (3) post-tilt compression (2 stress axes horizontal) at sites 3, 6 and 18 (Figure 11). As NNE-trending compression was locally recorded before, during and after the tilt of the growth strata we conclude that this reverse and locally strike-slip faulting regime prevailed during the deposition of the UAFS, and therefore during the formation of the Sainte-Victoire Mountain and Roques Hautes thrust systems.

5.2. Pyrenean Compressional Stress Regime in the Arc Basin

[40] To characterize the outer compressional stress regime of the western Sainte-Victoire System, we measured additional fault data in Late Cretaceous to Eocene series of the northern margin of the Arc Basin (Figure 11). We found reverse and strike-slip faults corresponding to NNE-trending compression in the west (sites 14, 15, 16, and 17), and a NNW-trending compression (sites 8, 9, 10, 11, 12 and 13) in the east. As a difference with the sites in the growth strata (black arrows in Figure 11), we cannot directly date this outer deformation. However, at site 13, the morphology of the fault surfaces indicates that faulting occurred during the lithification of the limestones [e.g., *Montenat et al.*, 1997] suggesting that this faulting occurred during Lutetian. Thus, our fault kinematic analysis displays evidence for a Lutetian compressional stress regime acting at the northern margin of the Arc Basin, characterized by an average N-trending $\sigma 1$ with arcuate local $\sigma 1$ varying from NNE to NNW. We interpret this fan-shaped stress pattern as resulting from the S-vergent thrusting of the western Sainte-Victoire System, acting as an indenter within the Arc Basin. Therefore, our cross sections, that trend N-S, can be restored.

5.3. Oligocene and Alpine Deformations in the Sainte-Victoire System

[41] In the western Sainte-Victoire System, Pyrenean thrusts and folds are cut by WNW-dipping normal faults (Figure 11). In the Roques Hautes area, the normal throws are up to several tens of meters. The fault slip analysis along the Roques Hautes normal faults reveals an E-trending extension (Figure 13a). The dip-slip normal faults cut deformed growth strata of the LAFS and UAFS, demonstrating that the extension occurred after the Pyrenean compression [*Hippolyte et al.*, 2012]. This E-trending extensional regime can be correlated with the opening of the West European rift system during the Oligocene [*Hippolyte et al.*, 1993]. In addition, although the Tortonian marine sequences of the Bibemus Plateau are slightly tilted [e.g., *Chorowicz and Ruiz*, 1984], only one strike-slip fault, cutting the basal wave-cut platform with an offset of 20 cm, could be found (Figure 13b). Moreover, the Tortonian sequence seals the Pyrenean and Oligocene structures (Figure 2). Thus no significant deformation occurred during the Oligocene extension and Alpine compression in the study area, showing that the growth of the Sainte-Victoire System was essentially related to the ~N-trending Pyrenean compression.

6. Structural Model of the Sainte-Victoire System: Balanced and Restored Cross Sections

[42] Field data and precise surface mapping combined with available geophysical data (see description below) form the basis for the construction of four balanced cross sections of about 30 km-long across the Sainte-Victoire System from the northern Rians Basin to the southern Arc Basin (Figure 2). Surface data were digitalized in three-dimensions using MapInfo and Vertical Mapper GIS softwares, and the 30 m ASTER (*Advanced Spaceborne Thermal Emission and Reflection Radiometer*) GDEM (*Global Digital Elevation Model*). Then, these data were exported in "2DMove" structural modeling and analysis software. The balanced cross sections were constructed according to thrust tectonic concepts [e.g., *Dahlstrom*, 1969; *Boyer and Elliott*, 1982; *Suppe*, 1983; *Suppe and Medwedeff*, 1990; *Mitra*, 2002; *Shaw et al.*, 2005]. The sections were restored on the basis of the "2DMove flexural slip algorithm" which allows maintaining bed lengths parallel to template line corresponding to aerial erosional surface related to the Durance uplift [e.g., *Masse and Philip*, 1976], and the area of the unfolded unit. The cross sections were restored considering the template line as flat (corresponding approximately to the top of the Early Cretaceous marine series), and pinned in the Rians Basin. In general, a local pin line is used for each thrust. According to our fault slip analysis (see chapter 5), the cross sections are parallel to the ~N-trending Pyrenean tectonic transport, and located far from main transverse structures (e.g., Bau Roux and Bau de Vespres structures; Figures 5b and 10a) to avoid out-of-plane displacement. The Concors, Ligourès and Keyrié structures are oblique (N120°E) with respect to the ~N-trending compression direction (Figure 2).

[43] The deep geometry of the Sainte-Victoire System is still a debate [*Tempier*, 1987; *Biberon*, 1988; *Roure and Colletta*, 1996]. Variations in depth of the base of synclines can be used to localize basement faults on the balanced cross sections [*Molinaro et al.*, 2005]. Also, to constrain the geometry of the basement-cover interface and the structural style in depth, we used the Jouques well drilled in the northern Rians Basin, combined with available geophysical data (seismic refraction and reflection) [see *Biberon*, 1988, and references therein] (Figure 2). The basement-cover interface is found at ~2 km of depth beneath the northern Rians Basin (Jouques well; Figure 2).

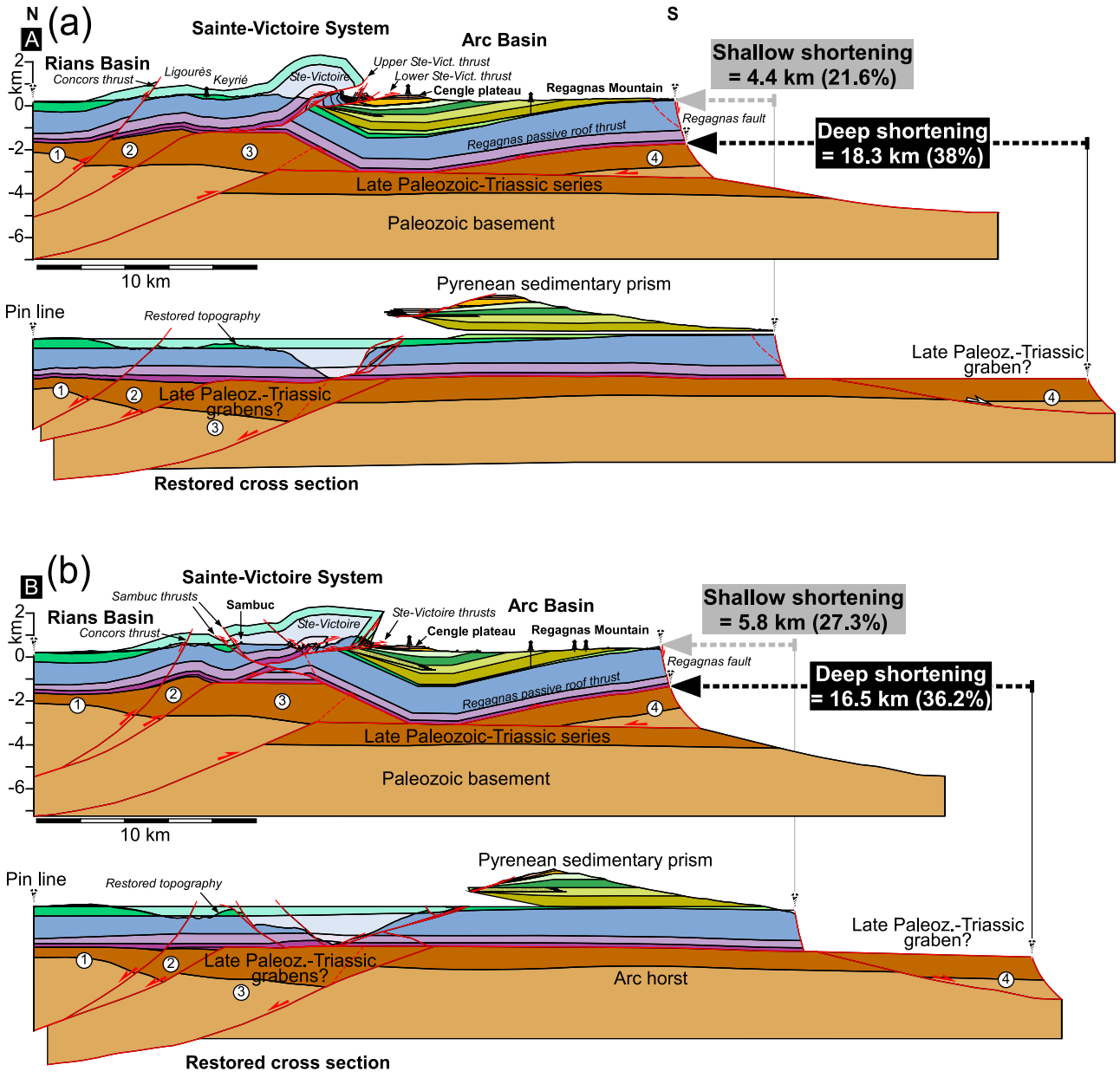

Figure 14. Balanced and restored cross sections across the Rians Basin, Sainte-Victoire System and Arc Basins. For location and legend, see Figure 2. Restored cross sections were obtained by flattening top of the Early Cretaceous marine series. (a) Cross section A. (b) Cross section B. (c) Cross section C. (d) Cross section D. The deep thick-skinned structure of the western Sainte-Victoire System is modeled using three basement thrust sheets, labeled 1, 2 and 3 and respectively localized beneath the Concors, Ligourès and Sainte-Victoire anticlines. These basement thrust sheets feed the slip of the western Sainte-Victoire System. Slip of basement thrust sheet 4 localized beneath Regagnas Mountain is mainly transferred in the S-vergent Regagnas passive roof thrust. In cross sections C and D, thrust sheet 4 localized beneath Regagnas Mountain feeds the slip of the eastern thin-skinned Sainte-Victoire System.

In other parts of the study area, seismic refraction data indicate a basement-cover interface located at a depth of ~3 km beneath the Rians Basin, Sainte-Victoire Mountain and southwestern Arc Basin, and down to ~4 km beneath the western Arc Basin (Figure 2). Thus, the study area shows significant spatial variations of the depth of the basement-cover interface: in the eastern domain, the geometry of the basement-cover interface is progressively deepening toward the south. In contrast, there is a strong structural evidence to suggest basement faulting beneath the western Sainte-Victoire System and southern Arc Basin [see *Biberon*, 1988].

6.1. Western Sainte-Victoire System

[44] Along balanced cross sections A and B (Figures 14a and 14b), the construction of the Arc, Kyerié and Rians synclines was conducted using surface and well data,

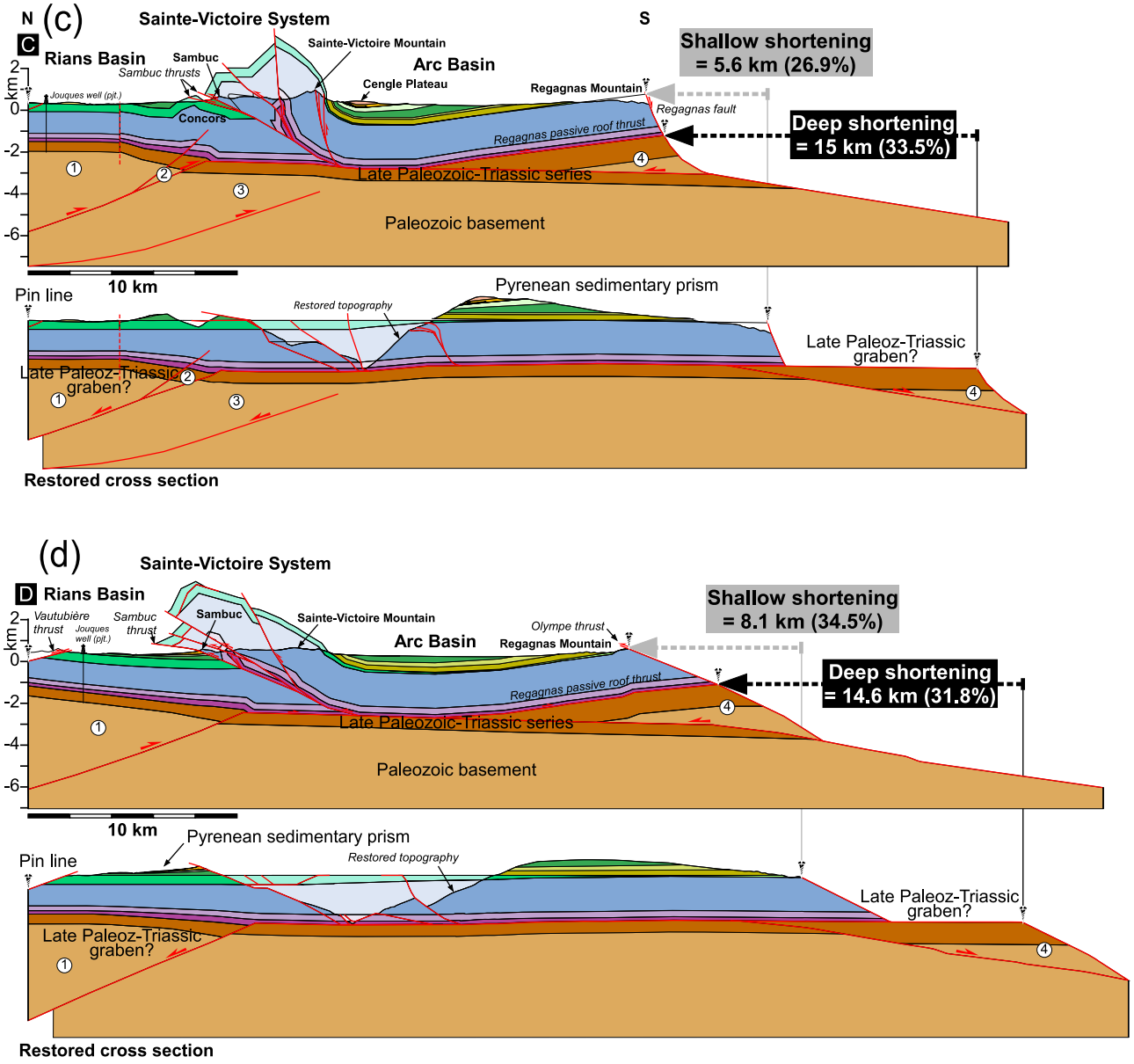

Figure 14. (continued)

assuming that the sedimentary pile is complete in the axis of each syncline. Although the thickness of the sedimentary series of the Arc syncline is not precisely constrained at depth, we modeled the regional basal décollement above Triassic series at a depth of ~4 km beneath the Arc syncline. In contrast, this basal décollement is located ~1.2 km and ~1.7 km beneath the Keyrié and Rians synclines, respectively. In the Rians Basin, seismic reflection and well data suggest no décollement above Triassic series [see *Biberon*, 1988]. Seismic refraction data throughout the western study area suggest that the basement is faulted and uplifted below the Sainte-Victoire System. The approximate depth of basement-cover interface being located at ~3 km and ~4 km beneath the western Sainte-Victoire System and the Arc syncline, respectively, we can estimate the presence of ~1.7 km-thick strata below the Sainte-Victoire and less than 900 m-thick strata below the Arc Basin. Below the northern Rians syncline, the Jouques well provides evidence for ~500 m-thick of Triassic series directly overlying the Hercynian basement. Although the Mesozoic regional datum of the Sainte-Victoire System is uplifted above those of the Arc Basin, *Roure and Colletta* [1996] suggested that the Sainte-Victoire System accommodates the inversion of a hypothetical Permian basin localized below the Arc Basin. However, our geometrical interpretation is more consistent with the presence of a S-thickening sedimentary wedge presumably bounded by a master N-dipping basement fault below the western Sainte-Victoire System. This wedge would be composed of Triassic strata and also probably Late Paleozoic (Carboniferous to Permian) strata [*Toutin-Morin et al.*, 1992]. North of the western Sainte-Victoire System, oblique ESE-trending structure of the Concors is inferred to

reactivate an older ESE-trending structural grain combined with abrupt thickness changes in the Late Paleozoic-Triassic sedimentary pile. We propose that this system extends below the western Sainte-Victoire System. The uplift of the western Sainte-Victoire System would be thus primarily produced by the tectonic inversion of a Late Paleozoic-Triassic half graben system. This inheritance explains the structural culmination of the western Sainte-Victoire System with respect to the southern Arc Basin. In our construction, we modeled that the inherited normal faults connect onto a subhorizontal mid-crustal detachment at a depth of ~7–8 km beneath the Rians Basin (Figures 14a and 14b).

[45] In details, the deep thick-skinned structural geometry below the western Sainte-Victoire System can be modeled using three basement thrust sheets, named 1, 2 and 3 and respectively localized beneath the Concors, Ligourès and Sainte-Victoire anticlines (Figures 14a and 14b). The construction of cross sections A and B shows that the Rians Basin was transported southward above upper horse 1. The slip of horse 1 was accommodated by the Concors thrust. The Ligourès anticline was transported southward above the intermediate horse 2. The southern basement ramp of horse 3 bounds the inverted half graben system. According to seismic refraction data and the construction of cross sections, this master fault is inferred to produce ~1 km of basement uplift below the Sainte-Victoire System with respect to the Arc Basin. The slip of the lower horse 3 was passively accommodated by a passive roof thrust as a deep intercutaneous tectonic wedge, propagating southward [*Shaw et al.*, 2005]. The upper S-vergent Sainte-Victoire thrust system connects down onto the deep passive roof thrust of horse 3, defining an upper north-directed intercutaneous wedge. This "zigzag" thrust array is typical of hinge wedge fold-accommodation faults defined by *Mitra* [2002].

[46] Thus, the shortening of the western Sainte-Victoire System may only result in the structural thick-skinned inversion of Late Paleozoic-Triassic oblique structures. For example, the restoration of cross section A shows that the shortening within the western Sainte-Victoire thrust systems and Arc Basin (~4470 m) is greatly balanced by the shortening (~4350 m) of basement horses 2 and 3 (~3% of shortening differences between basement and cover).

[47] South of the Arc Basin, Regagnas Mountain exhibits similar oblique ESE-trending structural grain like the Concors structure (Figure 2). The long planar geometry of the southern limb of the Arc syncline can be explained as resulting from an intercutaneous thrust wedge below Regagnas Mountain. According to seismic refraction data, we propose that this thrust sheet (named 4 in Figure 14) is composed of basement rocks overlain by ~1 km-thick Late Paleozoic-Triassic strata. Restored cross sections show that the northern and southern edges of the Arc Basin correspond to extensional structures separated by a central high during Late Paleozoic-Triassic times (Figure 14).

6.2. Eastern Sainte-Victoire System

[48] The construction of balanced cross sections C and D (Figures 14c and 14d) suggests that the shortening within the eastern Sainte-Victoire System can be essentially accommodated by the northward propagation of thin-skinned thrusts. As for the western Sainte-Victoire System, the main décollement level in cover occurs in the upper part of the Triassic series, probably at the base of the Rhaetian series. The cross section construction reveals that the décollement level is located at ~2.8 km of depth at the footwall of the Sainte-Victoire System, and dips gradually toward the south. In the Rians Basin, the Jouques well shows little basement uplift with respect to the Arc Basin (Figures 14c and 14d). This uplift is interpreted as the eastern continuation of Concors structure and deep basement thrust sheets. Interestingly, as confirmed by the geophysical data (see above), this structural style is not accompanied by a strong involvement of the thick-skinned structures. As for the western cross sections, the geometry of the southern limb of the Arc syncline can be explained as resulting from an intercutaneous thrust sheet below Regagnas Mountain. The restoration of the balanced cross sections suggests that the shortening within the eastern Sainte-Victoire System is mostly attributed to feed slip from southern Regagnas thrust sheet 4 (Figures 14c and 14d.

6.3. Shortening Assessment

[49] The calculated shortening magnitudes that we propose are minimum values owing to the uncertainty involved in calculating the amount of thrust displacement where hanging wall cut-offs are removed by erosion [see *Judge and Allmendinger*, 2011 for more details]. Two different horizontal shortening amounts have been calculated: (1) the total horizontal shallow shortening of the Sainte-Victoire System and (2) the total horizontal deep shortening across the Rians and Arc Basins, including deep basement thrust sheet 4 (Figure 14). The restoration results of the four balanced cross sections are plotted in Figure 15. The results show that the shallow shortening amount of the Sainte-Victoire System changes from ~5 km (i.e., ~25%) to the west (cross sections A and B), to ~8 km (i.e., ~34%) to the east (cross section D), which corresponds to an eastward increase of the shortening of about 38%. In contrast, we observe a westward increase of ~16% of the deep shortening, from 14.6 km (i.e., 31.8%) to the east to 18.3 km (i.e., 38%) to the west. Assuming that the shortening is internally compensated within each of the balanced cross sections, the calculated difference between the Sainte-Victoire System shortening and the deep shortening (Figure 15) has to be accommodated by the S-vergent Regagnas passive roof thrust (Figure 14). The shortening amount of the Regagnas passive roof thrust indicates a decrease of the shortening toward the east, from ~14 km to 6.5 km (Figure 15).

[50] The total shallow shortening in the eastern Sainte-Victoire System (cross section D) is in accordance with the amounts of shortening (~8 km) calculated by *Biberon* [1988]. However, our calculated surface shortening values for the western Sainte-Victoire System (cross sections A and B) are three-times smaller than those calculated by *Biberon* [1988] (~13 km). This difference can be explained by our thick-skinned interpretation of the deep oblique structures of the western Sainte-Victoire System (Figures 14a and 14b).

7. Discussion

7.1. Paleozoic Structural Inheritances in Provence

[51] Several studies pointed out that the control exerted by the preexisting basement structures was the most important

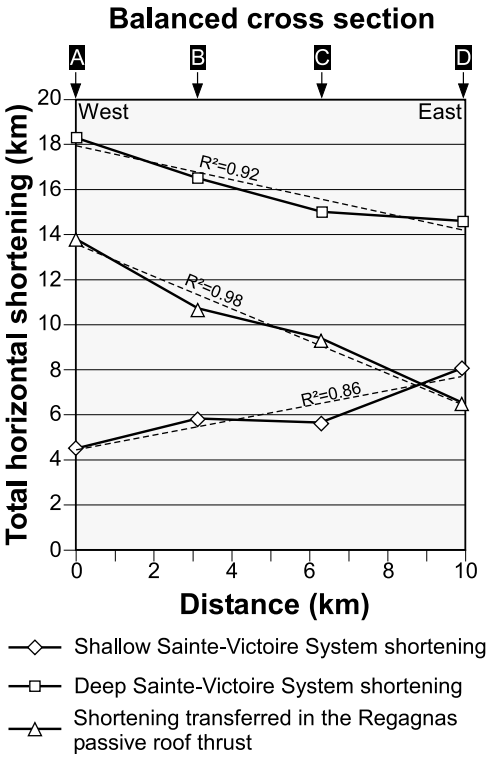

Figure 15. Plots of total horizontal shortening for each balanced cross section. The shallow horizontal shortening of the Sainte-Victoire System is calculated using pin lines in the northern edge of Rians Basin and the southern edge of the Arc Basin (see Figure 14). The calculation of the deep horizontal shortening includes the basement shortening of thrust sheet 4 located below Regagnas Mountain. See details in the text.

control process on the development of many fold-and-thrust belts on Earth [e.g., *Muñoz*, 1992; *Roure and Colletta*, 1996; *Colletta et al.*, 1997; *Lacombe and Mouthereau*, 2002; *Mora et al.*, 2006; *Saura and Teixell*, 2006]. The involvement of inherited basement structures within the Pyrenean foreland of Provence remains controversial or insufficiently constrained [e.g., *Tempier*, 1987; *Roure and Colletta*, 1996]. Our study highlights some important implications of the Paleozoic inheritances for the tectonic evolution of the Pyrenean foreland of Provence.

[52] Preserved N- and ESE-trending Late Paleozoic to Triassic extensional structures inherited from the fragmentation of Gondwana, are essentially exposed in the Maures Massif-Tanneron (Figure 16) [e.g., *Arévian et al.*, 1979; *Delfaud et al.*, 1989; *Toutin-Morin et al.*, 1992; *Toutin-Morin and Bonijoly*, 1992]. These structures mainly correspond to half graben systems infilled by Late Carboniferous to Permian volcanoclastic continental sequences and Triassic fluvial series. The Concors anticline as well as the Vautubière Mountain, Vinon, Gréoux and other deep structures located below the Valensole Basin [e.g., *Dubois and Curnelle*, 1978], show similar trend as Late Paleozoic grain of the northern Maures Massif-Tanneron (Figure 16) [*Toutin-Morin and Bonijoly*, 1992]. These structural coincidences lead us to propose that the structure of the western Sainte-Victoire System may result from the inversion of Late Paleozoic half graben systems with ESE-trending basement faults. Our structural model also supports that lower Triassic sequences presumably filled the half graben system [*Toutin-Morin et al.*, 1992].

[53] Subsurface and seismicity data from northern Provence provide evidence for the implication of the basement within the shortening of the Pyrenean/Alpine foreland of Provence. For example, the trace of the Middle Durance fault (prolongated with the southern Aix-en-Provence fault) is interpreted as overprinting a NNE-trending basement grain of Late Paleozoic age [*Arthaud and Matte*, 1975] (Figure 16). This fault system separates two domains: a western domain where the thickness of the Mesozoic-Cenozoic sedimentary pile ranges between 6 km and more than 10 km and an eastern domain where the average thickness is ~2 km (Sainte-Victoire System area, Figure 16) [*Ménard*, 1980]. West of the Middle Durance fault, the main part of the deep-located seismic events related to the Alpine shortening are mostly located at the basement-sedimentary cover interface (less than 11 km) [*Cushing et al.*, 2007] which could illustrate a basement-cover detachment (Figure 16) [*Terrier et al.*, 2008; *Molliex et al.*, 2011]. East of the Middle Durance fault, the presence of seismic events below the Valensole Basin at a similar depth than to the west shows active basement faults. In fact, the heterogeneity of the Mesozoic-Cenozoic sedimentary pile on both sides of the Middle Durance/Aix-en-Provence fault system may have controlled the structural style during subsequent compressions. West of the fault system, the Pyrenean and Alpine compressive stages resulted in the extrusion of the basin infill without reactivation of the normal faults (thin-skinned tectonic style). On the contrary, these faults are inverted east of the Middle Durance fault like beneath the Sainte-Victoire System (thick-skinned tectonic style). This explains why although seismic events are located at similar depths, basement involvement is different at both sides of the Middle Durance/Aix-en-Provence fault system (Figure 16).

7.2. Structural Wedging and Shortening Partitioning

[54] The structural inversion in the northern margin of the Arc Basin can be interpreted using structural wedge models as defined by *Shaw et al.* [2005]. Our structural model of the western Sainte-Victoire System (Figures 14a and 14b) is composed of two stacked wedges: a lower wedge composed of thick Late Paleozoic-Triassic rift sequences, propagating southward, and a shallower wedge developed within the Mesozoic-Cenozoic sedimentary cover, propagating northward. The geometry and kinematics of the proposed lower intercutaneous wedge are similar to those described by sandbox analog models [*Roure and Colletta*, 1996] and natural examples in the Rocky Mountains of Canada [*Price*, 1986] and in the northern Amadeus Basin of Central Australia [*Flöttmann and Hand*, 1999]. However, our model suggests a coeval motion of the lower and upper wedges (Figures 14a and 14b). These "zigzag" geometry [*Mitra*, 2002] and kinematics are also similar to natural examples described in the Andes of Chile [*Amilibia et al.*, 2008], Junggar Basin of China [*Guan et al.*, 2009] and the southern foreland of Tunisian Atlas [*Said et al.*, 2011]. The formation of the upper wedge might result from the absence of a mechanically weak detachment horizon within Triassic series north

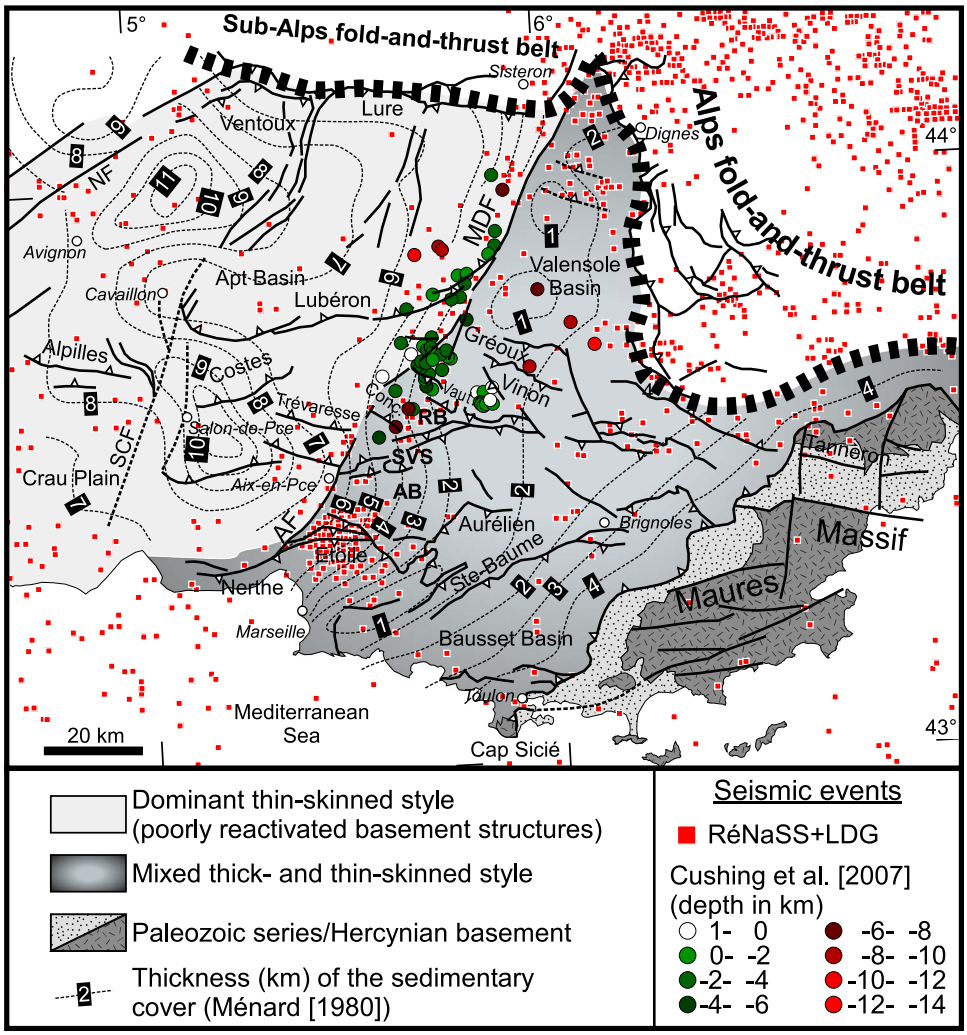

Figure 16. Structural map illustrating the structural style of the Pyrenean/Alpine fold-and-thrust belt of Provence. Thickness of the Mesozoic-Cenozoic sedimentary cover is from *Ménard* [1980]. Red squares correspond to seismic event data from "*Réseau National de Surveillance Sismique*" (*RéNaSS*) and "*Laboratoire de Détection Géophysique*" (*LDG*) (1980–2010). Location and depth (km) of the best located seismic events recorded by the Durance network from 1999 to 2006 are from *Cushing et al.* [2007]. The area located west of the Aix-en-Provence-Middle Durance fault system is characterized by a thin-skinned tectonic style with poorly reactivated basement faults. In contrast, the area located to the east shows a pronounced thick-skinned tectonic style. Present-day seismic events [*Cushing et al.*, 2007], related to the Alpine compression, are approximately located at similar depths on both sides of the Middle Durance fault, suggesting active thin-skinned thrusting to the west and basement thrusting to the east. This along-strike contrasted tectonic style may result from heterogeneity in terms of thickness in the Mesozoic-Cenozoic sedimentary cover: thick (∼10 km) to the west and thin (∼2 km) to the east. NF: Nîmes fault. SCF: Salon-Cavaillon fault. AF: Aix-en-Provence fault. MDF: Middle Durance fault. SVS: Sainte-Victoire System. RB: Rians Basin. AB: Arc Basin.

of horse 3 [*Biberon*, 1988], that could prevent the propagation of the deformation northward (Figures 14a and 14b).

[55] At the scale of the Rians and Arc Basins, balanced cross section results show pronounced along-strike variations in terms of shallow and deep shortenings (Figure 15). The amount of shortening by thick-skinned reactivation mainly occurred in the western Sainte-Victoire System, whereas thin-skinned thrusting was more important in the east (Figures 14 and 15). The restoration of balanced cross section A shows that the structure of the western Sainte-Victoire System requires no feed slip from the south. The upper and deep thrust systems of the western Sainte-Victoire System are a single southward migrating system, progressively decoupled by the upper thin-skinned tectonic wedge (Figure 14a). In the southern part of the Arc Basin, the emplacement of horse 4 is associated with the uplift of Regagnas Mountain. We propose that the S-vergent western Sainte-Victoire System played the role of buttress. This implies that the large displacement associated with horse 4 was entirely translated southward to its roof thrust

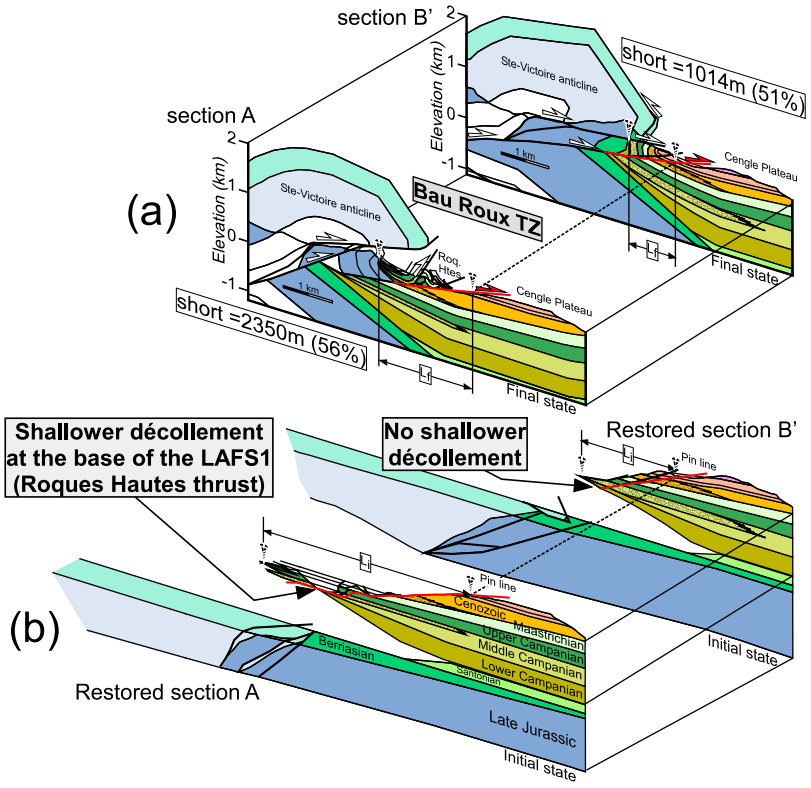

Figure 17. Kinematics of the Bau Roux transverse structure. (a) Details of balanced cross sections A and B′ located on both sides of the local Bau Roux transverse zone. For location, see Figure 2. (b) Restored cross sections. Li: Initial length; Lf: Final length; short: Shortening. Cross section restoration shows larger shortening in the west (2350 m) than in the east (1014 m) as a result from the existence of a shallower décollement level at the base of the middle Campanian breccias of the LAFS1 in the Roques Hautes area.

(Regagnas passive roof thrust) along balanced cross section A. Along balanced cross sections C and D, the shortening of horse 4 has been partly transferred northward to feed the slip of the entire growth of the eastern thin-skinned Sainte-Victoire System (Figure 15).

7.3. Transverse Structures

[56] The pre-existing basement structures and lateral heterogeneities in the mechanical stratigraphic pile may have strong controls on the location and development of transverse structures. In the Sainte-Victoire System area, we observe complex along-strike relationship between folds and faults of different trends (Figure 2). Geometric and structural evidences suggest that the Sainte-Victoire Mountain structure is laterally bounded by two major transverse systems: the western Bau Roux and the eastern Bau de Vespres transverse systems (Figures 10 and 12).

[57] The western Bau Roux transverse structure marks the end of the N-vergent eastern Sainte-Victoire System. It corresponds to a westward imbricate of four lateral ramps and minor sinitral strike-slip faults (Figure 12a). The displacement along the ramps is accommodated by a NNE-trending fold mainly formed by Danian breccias of the UAFS (Figure 12b). Figure 17 shows details of the thrust systems located on the southern flank of the Sainte-Victoire anticline of cross sections A and B′. Interestingly, the local restoration of these cross sections shows that a differential shortening has been accommodated on both sides of the Bau Roux transverse structure: ∼2.3 km in section A and ∼1 km in section B′. Field data suggest that the development of the Bau Roux transverse structure mainly results from the existence of a major shallow décollement level at the base of the middle Campanian breccias of the LAFS1 in the Roques Hautes area (Figures 12 and 17). The shortening has been preferentially transferred southward onto this shallower décollement and accommodated by the Roques Hautes thrust systems. Eastward, no décollement level at the base of the middle Campanian breccias has been observed in the field and all the deformation has been accommodated by the lower Sainte-Victoire hanging wall ramp. According to these observations, the Roques Hautes imbricate can be considered as a tectonic half-tectonic window under the low-angle upper Sainte-Victoire thrust (Figure 17).

[58] The eastern Bau de Vespres transverse structure marks the end of the S-vergent western Sainte-Victoire System. In this zone, middle Campanian to Maastrichtian breccias of the LAFS were transported southward along imbricated lateral ramps (Figure 10). The displacement along these lateral ramps decreases rapidly eastward. Thus, we propose that the kinematics link between the western S-vergent and eastern N-vergent Sainte-Victoire Systems were associated to the development of a regional relay zone (Sainte-Victoire

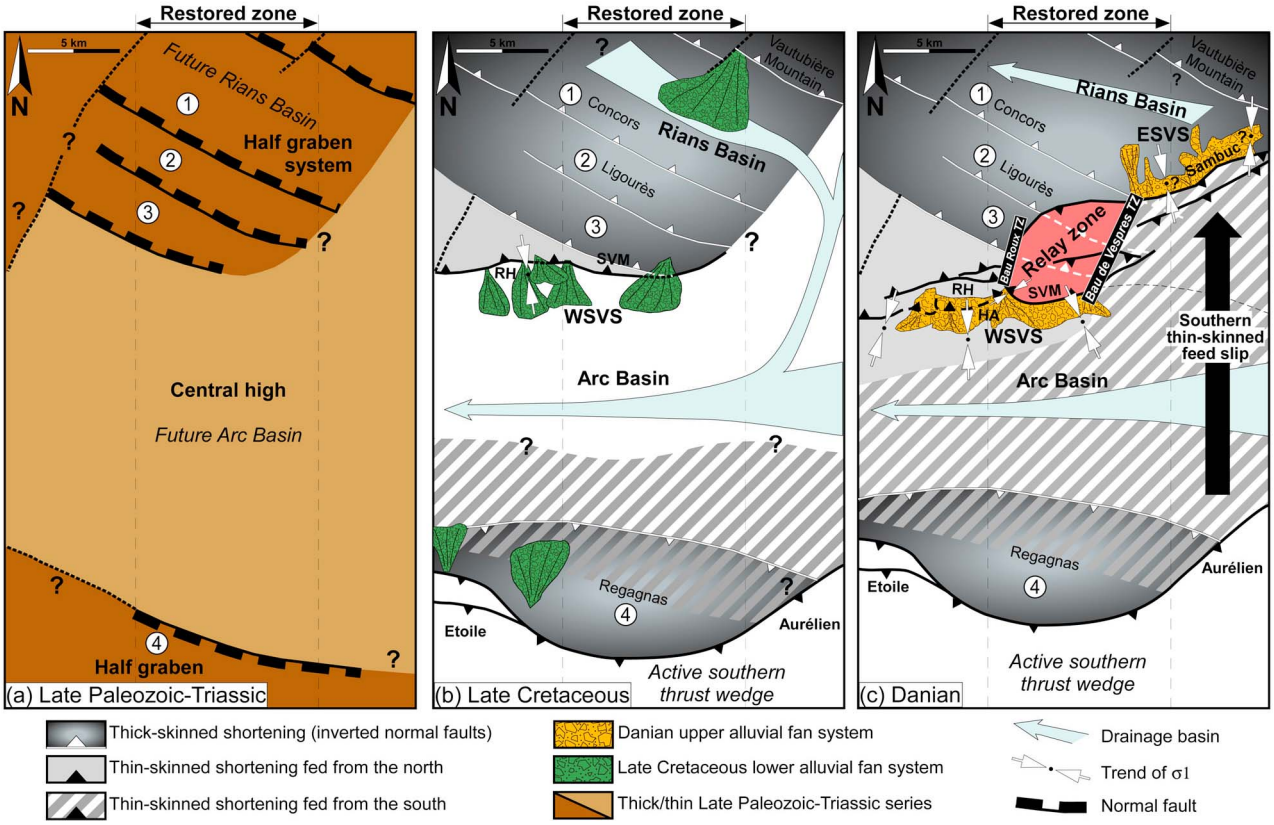

Figure 18. Schematic evolutionary model for the Sainte-Victoire System. (a) Initial Late Paleozoic-Triassic basin geometry. Labels 1, 2, 3 and 4 correspond to basement structures of Figure 14. (b) Growth of the western Sainte-Victoire System (WSVS) started in Late Cretaceous (Campanian-Maastrichtian) as a result of the reactivation of oblique ESE-trending Late Paleozoic-Triassic extensional structures. During the inversion, the structural reliefs were progressively eroded, providing the source for the LAFS at the Vautubière Mountain, Sainte-Victoire Mountain (SVM)/Roques Hautes (RH) and Etoile thrust fronts. The Arc and Rians Basins were hydrologically connected eastward [*Cojan*, 1993]. (c) The formation of the structural relief of the eastern Sainte-Victoire System (ESVS) and the continuous growth of the western Sainte-Victoire System were recorded by UAFS at the Sambuc thrust front and Harmelins (HA)/Sainte-Victoire Mountain thrust fronts, respectively. Growth of the eastern Sainte-Victoire System only started during Danian as a result of a thin-skinned shortening transfer from the southern basement Regagnas thrust sheet. The kinematics link between the western and eastern Sainte-Victoire Systems was associated to the development of a regional relay zone (red area) between the Bau Roux and Bau de Vespres transverse zones (TZ). White arrows show the direction of maximum (σ1) compressional stress regime, ranging from NNE to NNW. See more details in the text.

Mountain) between the Bau Roux and Bau de Vespres transverse structures (Figure 18). This regional relay zone is consistent with stress regime perturbations observed between the eastern and western Sainte-Victoire Systems, the direction of σ1 ranging from NNE to NNW.

7.4. Deformational History

[59] Two contrasted models describe the thrust sequence in forelands at the orogen scale: the first model consists in a classical forward sequence in which the sedimentary cover detached first and basement thrusting occurs second at depth; the second model consists in a foreland-to-hinterland sequence in which foreland basement reactivations occur first and the thin-skinned shortening propagates second [e.g., *Lacombe and Mouthereau*, 2002; *Hilley et al.*, 2005; *Mora et al.*, 2010]. Arguments for each model mainly come from geometric evidence and/or growth strata [*Boyer*, 1992; *Hain et al.*, 2011].

[60] The presence of syntectonic foreland basin sediments in the Sainte-Victoire System combined with balanced cross sections allows us to precisely assess the temporal and spatial deformation evolution with respect to the structural style (Figure 18). Growth strata show that the onset of deformation started diachronically along-strike. In the western Sainte-Victoire System, middle Campanian growth strata of the LAFS1 suggest that the thick-skinned structures have presumably been reactivated at least since the middle Campanian and remained active through the Maastrichtian (LAFS2)-Danian (UAFS) period, and probably until the Lutetian (~43 Ma) (see above chapter 5.3). Besides, field

data and balanced cross section constructions show a major pinchout of the continental lower Campanian sequences onto the northern limb of the Arc syncline, associated to the emplacement of the lower, S-directed intercutaneous wedge (Figures 14a and 14b). This suggests that the tectonic inversion and growth of the western Sainte-Victoire System rather started during the lower Campanian (~83 Ma). Thus, the western thick-skinned Sainte-Victoire System recorded the early stages of development of the Pyrenean shortening in Provence and have focused a continuous deformation during ~40 Myr (i.e., between ~83 Ma and ~43 Ma) (Figure 18). A similar example of long-living structure has been described in the Subandes of Colombia by *Mora et al.* [2010]. Based on the model by *Mora et al.* [2010], we propose that Late Paleozoic-Triassic basement faults orientation enhanced their reactivation under the Pyrenean stress regime, focusing a continuous deformation in the outer foreland of Provence, a different mechanism from classical thrust wedge mechanics [e.g., *Davis et al.*, 1983]. In the eastern Sainte-Victoire System, no breccia series or growth strata are found in the Late Cretaceous series (Figure 14d). Although these series may have been eroded, the occurrence of Danian growth strata of the UAFS in the Rians Basin demonstrates that the lateral thin-skinned shortening of the eastern Sainte-Victoire System started significantly later (~65 Ma). Thus, the eastern Sainte-Victoire System mainly results from the N-vergent migration of the thin-skinned thrust front during the Danian and probably until Eocene times (i.e., ~22 Myr) (Figure 18). This is in agreement with *Cojan* [1993] paleogeography reconstructions within the Arc and Rians Basins. Indeed, the stratigraphic correlations in Maastrichtian/lower Paleocene series infilling these basins clearly show that these basins were hydrologically connected during the Late Cretaceous (Figure 18).

7.5. Implication for Orogen Scale Shortening

[61] The deep shortening values (15–18 km) calculated for the Sainte-Victoire System are not representative for the convergence rate between the Corsica-Sardinia block and Eurasia during Late Cretaceous to Eocene. However, our calculation does not include the northern Vautubière Mountain and southern Etoile/Sainte-Baume structures (Figures 1a and 18) also associated with Late Cretaceous/Paleocene growth strata [e.g., *Corroy and Philip*, 1964; *Aubouin and Chorowicz*, 1967; *Cojan*, 1993; *Leleu et al.*, 2009]. The shortening values of the Sainte-Victoire System are weak at a regional scale, however, combined with shortening accommodated by synchronous structures of similar characteristics in the Provence foreland may result in a significant increase of cumulated continental shortening at the Pyrenean-Provence orogen scale.

8. Conclusions

[62] Structural, growth strata and fault slip analyses, together with the construction of four 30 km-long balanced cross sections, allow us to constrain the along-strike structural architecture, kinematics and timing of the deformation of the Sainte-Victoire System and adjacent syntectonic Arc and Rians Basins. The main conclusions are as follows:

[63] 1. The Sainte-Victoire System is divided into two structural domains: an eastern domain governed by a N-vergent thin-skinned tectonic style above Triassic series; a western domain of mixed S-vergent thick- and thin-skinned tectonic style with tectonic inversion of Late Paleozoic-Triassic half graben system.

[64] 2. The along-strike bi-vergence of the Sainte-Victoire System was accommodated by a regional relay zone bounded by the Bau de Vespres transverse structure to the east and the Bau Roux transverse structure to the west. This relay zone was responsible for compressional stress regime perturbations, the direction of $\sigma 1$ ranging from NNE to NNW, during the growth of the Sainte-Victoire System.

[65] 3. At a local scale, the shallow N-S shortening is ~5 km (~25%) and ~8 km (~34%) in the western and eastern Sainte-Victoire System, respectively. At a regional scale, the tectonic inversion of the Sainte-Victoire System and the Arc Basin recorded a deep shortening of the order of 15–18 km (~34%).

[66] 4. Inherited basement faults of the Provence area had an adequate for compressional reactivation during the Late Cretaceous-Eocene Corsica-Sardinia block and Eurasia collision. They recorded the early stages (Campanian) of development of the Pyrenean shortening in Provence and have focused a continuous deformation during ~40 Myr in the western Sainte-Victoire System. Although the shortening magnitudes of the Sainte-Victoire System remain weak at local scale, other foreland structures similar to the Sainte-Victoire System were active simultaneously across foreland basin, resulting in a significant increase of cumulated continental shortening at the Pyrenean-Provence orogen scale.

[67] **Acknowledgments.** This study has been developed within the "*Cadarache Seismic Hazard Integrated Multidisciplinary Assessment-Commissariat à l'Energie Atomique*" program supervised by F. Hollender and the "*Observatoire Hommes-Milieux*" du bassin minier de Provence (Fédération de recherche "*Ecosystèmes Continentaux et Risques Environnementaux*") program supervised by S. Robert. Midland Valley is acknowledged for providing academic license of "2DMove" for structural modeling. We thank M. Floquet, J. Philip, J.-M. Triat, S. Leleu, I. Cojan, Y. Dutour and T. Tortosa for their useful discussions. J. Fleury helped with the imagery processing. We acknowledge two anonymous reviewers for their comments and suggestions that greatly contributed to the improvement of the original manuscript.

References

Amilibia, A., F. Sàbat, K. R. McClay, J. A. Muñoz, E. Roca, and G. Chong (2008), The role of inherited tectono-sedimentary architecture in the development of the central Andean mountain belt: Insights from the Cordillera de Domeyko, *J. Struct. Geol.*, *30*, 1520–1539, doi:10.1016/j.jsg.2008.08.005.

Andreani, L., N. Loget, C. Rangin, and X. Le Pichon (2010), New structural constraints on the southern Provence thrust belt (France): Evidences for an Eocene shortening event linked to the Corsica-Sardinia subduction, *Bull. Soc. Geol. Fr.*, *181*, 547–563, doi:10.2113/gssgfbull.181.6.547.

Angelier, J. (1971), La partie septentrionale de la bande triasique de Barjol (Var), PhD thesis, 193 pp., Faculté des Sciences de Paris, Paris.

Angelier, J. (1990), Inversion of field data in fault tectonics to obtain the regional stress–III. A new rapid direct inversion method by analytical means, *Geophys. J. Int.*, *103*, 363–376, doi:10.1111/j.1365-246X.1990.tb01777.x.

Angelier, J., A. Tarantola, B. Valette, and S. Manoussis (1982), Inversion of field data in fault tectonics to obtain the regional stress, I, Single phase fault populations: A new method of computing the stress tensor, *Geophys. J. R. Astron. Soc.*, *69*, 607–621, doi:10.1111/j.1365-246X.1982.tb02766.x.

Arévian, A., N. Toutin, H. Rousseau, R. Campredon, and R. Dars (1979), Les séries continentales du Permien du Var, *Bull. Bur. Rech. Geol. Min.*, *1*, 31–43.

Arlhac, P., et al. (1970), Geological map of the France, *Map 995*, scale 1:50,000, Bur. de Rech. Geol. et Min., Orléans, France.

Arthaud, F., and P. Matte (1975), Les décrochements tardi-hercyniens du sud-ouest de l'Europe. Géometrie et essai de reconstitution des conditions

de la déformation, *Tectonophysics*, *25*, 139–171, doi:10.1016/0040-1951(75)90014-1.

Arthaud, F., and M. Seguret (1981), Les structures pyrénéennes du Languedoc et du golfe du Lion (Sud de la France), *Bull. Soc. Geol. Fr.*, *23*, 51–63.

Aubouin, J., and J. Chorowicz (1967), Le chevauchement sud-Provençal: De l'Etoile à la Sainte-Baume, *Bull. Soc. Geol. Fr.*, *7*, 600–608.

Baroux, E., N. A. Pino, G. Valensise, O. Scotti, and M. Cushing (2003), Source parameters of the 11 June 1909, Lambesc (southern France) earthquake: A reappraisal based on macroseismic, seismological and geodetic observations, *J. Geophys. Res.*, *108*(B9), 2454, doi:10.1029/2002JB002348.

Bergerat, F. (1987), Stress field in the European platform at the time of Africa–Eurasia collision, *Tectonics*, *6*, 99–132, doi:10.1029/TC006i002p00099.

Besson, D. (2005), Architecture du bassin rhodano-provençal miocène (Alpes, SE France), Relations entre déformation, physiographie et sédimentation dans un bassin molassique d'avant-pays, PhD thesis, 438 pp., Ecole des Mines de Paris, Paris.

Biberon, B. (1988), Mécanismes et évolution de chevauchements à vergences opposées. Exemple de la Montagne Sainte-Victoire, PhD thesis, 189 pp., Univ. Joseph Fourier, Grenoble, France.

Boyer, S. E. (1992), Geometric evidence for synchronous thrusting in the southern Alberta and northwest Montana thrust belts, in *Thrust Tectonics*, edited by K. R. McClay, pp. 377–390, Chapman and Hall, London, doi:10.1007/978-94-011-3066-0_34.

Boyer, S. E., and D. Elliott (1982), The geometry of thrust systems, *AAPG Bull.*, *66*, 1196–1230.

Butler, R. W. H., E. Tavarnelli, and M. Grasso (2006), Structural inheritance in mountain belts: An Alpine–Apennine perspective, *J. Struct. Geol.*, *28*, 1893–1908, doi:10.1016/j.jsg.2006.09.006.

Carey, E., and B. Brunier (1974), Analyse théorique et numérique d'un modèle mécanique élémentaire appliqué à l'étude d'une population de failles, *C. R. Acad. Sci. Paris*, *279*, 891–894.

Cassini G., M. Durand, and A. Ronchi (2003), Permian-Triassic continental sequences of northwest Sardinia and south Provence: Stratigraphic correlations and palaeogeographical implications, *Boll. Soc. Geol. It.*, *2*, 119–129.

Catzigras, F., E. Colomb, J. P. Durand, G. Guieu, C. Rousset, C. Tempier, D. Nury, and J. Rouire (1969), Geological map of the France, map of Aix-en-Provence, *Map 1021*, 2nd ed., scale 1:50,000, Bur. de Rech. Geol. et Min., Orléans, France.

Champion, C., P. Choukroune, and G. Clauzon (2000), La déformation post-Miocène en Provence occidentale, *Geodin. Acta*, *13*, 67–85, doi:10.1016/S0985-3111(00)00114-5.

Chardon, C., and O. Bellier (2003), Geological boundary conditions of the 1909 Lambesc (Provence, France) earthquake: Structure and evolution of the Trevaresse ridge anticline, *Bull. Soc. Geol. Fr.*, *174*, 497–510, doi:10.2113/174.5.497.

Chorowicz, J., and R. Ruiz (1984), La Sainte-Victoire (Provence): Observations et interprétations nouvelles, *Geol. Fr.*, *4*, 41–55.

Chorowicz, J., A. Mekarnia, and J.-P. Rudant (1989), Inversion tectonique dans le massif de la montagne Sainte-Victoire (Provence, France). Apport de l'imagerie Spot, *C. R. Acad. Sci. Paris*, *308*, 1179–1185.

Clauzon, G., J. Fleury, O. Bellier, S. Molliex, and L. Mocochain (2011), Tectonics and morphogenesis of northern Provence during the Miocene: A morphostructural study of the Luberon (Vaucluse), *Bull. Soc. Geo. Fr.*, *182*, 93–108.

Cojan, I. (1989), Discontinuité majeures en milieu continental. Proposition de corrélation avec des événements globaux (Bassin de Provence, S. France, Passage Crétacé/Tertiaire), *C. R. Acad. Sci. Paris*, *309*, 1013–1018.

Cojan, I. (1993), Alternating fluvial and lacustrine sedimentation: Tectonics and climatic controls (Provence Basin, S. France, Upper Cretaceous/Paleocene), *Spec. Publ. Int. Assoc. Sedimentol.*, *17*, 425–438.

Cojan, I., M. Renard, and L. Emmanuel (2003), Palaeoenvironmental reconstruction of dinosaur nesting sites based on a geochemical approach to eggshells and associated palaeosols (Maastrichtian, Provence Basin, France), *Palaeogeogr. Palaeoclimatol. Palaeoecol.*, *191*, 111–138, doi:10.1016/S0031-0182(02)00655-7.

Colletta, B., F. Roure, B. De Toni, D. Loureiro, H. Passalacqua, and Y. Gou (1997), Tectonic inheritance, crustal architecture, and contrasting structural style in the Venezuelan Andes, *Tectonics*, *16*, 777–794, doi:10.1029/97TC01659.

Corroy, G., and J. Philip (1964), Le brachyanticlinal des pics des Corbeaux, dans le massif de la Sainte-Baume (Var), *Bull. Soc. Geol. Fr.*, *7*, 560–563.

Corroy, G., C. Tempier, and J. P. Durand (1964), Evolution tectonique de la montagne Sainte-Victoire en Provence, *C. R. Acad. Sci. Fr.*, *258*, 1556–1557.

Coward, M. P. (1996), Balancing sections through inverted basins, *Geol. Soc. Spec. Pub.*, *99*, 51–77.

Cushing, M., O. Bellier, S. Nechtschein, M. Sébrier, P. Volant, A. Lomax, P. Dervin, P. Guignard, and L. Bove (2007), A multidisciplinary study of a slow-slipping fault for seismic hazard assessment: The example of the middle Durance fault (SE France), *Geophys. J. Int.*, *172*, 1163–1178, doi:10.1111/j.1365-246X.2007.03683.x.

Dahlstrom, C. D. A. (1969), Balanced cross sections, *Can. J. Earth Sci.*, *6*, 743–757, doi:10.1139/e69-069.

Davis, D., J. Suppe, and F. A. Dahlen (1983), Mechanics of fold-and-thrust belts and accretionary wedges, *J. Geophys. Res.*, *88*, 1153–1172, doi:10.1029/JB088iB02p01153.

Delfaud, J., N. Toutin-Morin, and R. Morin (1989), Un cone alluvial en bordure d'un basin intramontagneux: La formation permienne du Rocher de Roquebrune (bassin de Bas-Argens, Provence orientale), *C. R. Acad. Sci. Paris*, *309*, 1811–1817.

Dubois, P., and R. Curnelle (1978), Résultats apportés par le forage des Mées no. 1 sur le plateau de Valensole (Alpes-de-Hautes-Provence), *C. R. Soc. Geol. Fr.*, *4*, 181–184.

Durand, J. P., and C. Tempier (1962), Etude tectonique de la zone des breches du massif de Sainte-Victoire, dans la region du Tholonet, *Bull. Soc. Geol. Fr.*, *7*, 97–101.

Flöttmann, T., and M. Hand (1999), Folded basement-cored tectonic wedges along the northern edge of the Amadeus Basin, Central Australia: Evaluation of orogenic shortening, *J. Struct. Geol.*, *21*, 399–412, doi:10.1016/S0191-8141(99)00031-0.

Garcia, G., and M. Vianey-Liaud (2001), Dinosaur eggshells as biochronological markers in Upper Cretaceous continental deposits, *Palaeogeogr. Palaeoclimatol. Palaeoecol.*, *169*, 153–164, doi:10.1016/S0031-0182(01)00215-2.

Gattacceca, J., A. Deino, R. Rizzo, D. S. Jones, B. Henry, B. Beaudoin, and F. Vadeboin (2007), Miocene rotation of Sardinia: New paleomagnetic and geochronological constraints and geodynamic implications, *Earth Planet. Sci. Lett.*, *258*, 359–377, doi:10.1016/j.epsl.2007.02.003.

Gaviglio, P. (1985), A fault and stress field analysis in a coal mine (Gardanne, Bouches du Rhône, France), *Tectonophysics*, *113*, 349–366, doi:10.1016/0040-1951(85)90205-7.

Gaviglio, P., and J. F. Gonzales (1987), Fracturation et histoire tectonique du bassin de Gardanne (Bouches du Rhône), *Bull. Soc. Geol. Fr.*, *4*, 675–682.

Graciansky, P. C., and M. Lemoine (1988), Early Cretaceous tectonics in the southwestern French Alps: A consequence of North-Atlantic rifting during Tethyan spreading, *Bull. Soc. Geol. Fr.*, *5*, 733–737.

Guan, S., B. Li, D. He, J. H. Shaw, and Z. Chen (2009), Recognition and exploration of structural wedges: A case study in the southern margin of Junggar Basin, China, *Earth Space Frontiers*, *16*, 129–137.

Guieu, G., J. Philip, J.-P. Durand, D. Nury, and C. Redondo (1987), Le détritisme provençal du Crétacé moyen à l'Oligocène dans son cadre paleogéographique, structural et géodynamique, *Geol. Alp.*, *13*, 247–271.

Guignard, P., O. Bellier, and D. Chardon (2005), Géométrie et cinématique post-oligocène des failles d'Aix et de la moyenne Durance (Provence, France), *C. R. Geosci.*, *337*, 375–384, doi:10.1016/j.crte.2004.10.009.

Guyonnet-Benaize, C., J. Lamarche, J.-P. Masse, M. Villeneuve, and S. Viseur (2010), 3D structural modelling of small-deformations in poly phase faults pattern, Application to the Mid-Cretaceous Durance uplift, Provence (SE France), *J. Geodyn.*, *50*, 81–93, doi:10.1016/j.jog.2010.03.003.

Hain, M. P., M. R. Strecker, B. Bookhagen, R. N. Alonso, H. Pingel, and A. K. Schmitt (2011), Neogene to Quaternary broken-foreland formation and sedimentation dynamics in the Andes of NW Argentina (25°S), *Tectonics*, *30*, TC2006, doi:10.1029/2010TC002703.

Hilley, G. E., P. M. Blisniuk, and M. R. Strecker (2005), Mechanics and erosion of basement-cored uplift provinces, *J. Geophys. Res.*, *110*, B12409, doi:10.1029/2005JB003704.

Hippolyte, J.-C., J. Angelier, and F. Roure (1992), Les permutations de contraintes dans un orogène: Exemple des terrains quaternaires du sud de l'Apennin, *C. R. Acad. Sci. Paris*, *315*, 89–95.

Hippolyte, J.-C., J. Angelier, D. Nury, F. Bergerat, and G. Guieu (1993), Tectonic-stratigraphic record of paleostress time changes in the Oligocene basins of the Provence, southern France, *Tectonophysics*, *226*, 15–35, doi:10.1016/0040-1951(93)90108-V.

Hippolyte, J. C., F. Bergerat, M. B. Gordon, O. Bellier, and N. Espurt (2012), Keys and pitfalls in mesoscale fault analysis and paleostress reconstructions, the use of Angelier's methods, *Tectonophysics*, doi:10.1016/j.tecto.2012.01.012, in press.

Jorda, M., and M. Provansal (1992), La montagne Sainte-Victoire, Structure, relief, et morphogenèse antérieure au Postglaciaire, *Mediterranee*, *75*, 17–28, doi:10.3406/medit.1992.2750.

Judge, P. A., and R. W. Allmendinger (2011), Assessing uncertainties in balanced cross sections, *J. Struct. Geol.*, *33*, 458–467, doi:10.1016/j.jsg.2011.01.006.

Lacombe, O., and L. Jolivet (2005), Structural and kinematic relationships between Corsica and the Pyrenees-Provence domain at the time of the Pyrenean orogeny, *Tectonics*, *24*, TC1003, doi:10.1029/2004TC001673.

Lacombe, O., and F. Mouthereau (2002), Basement-involved shortening and deep detachment tectonics in forelands of orogens: Insights from recent collision belts (Taiwan, Western Alps, Pyrenees), *Tectonics*, *21*(4), 1030, doi:10.1029/2001TC901018.

Lacombe, O., J. Angelier, and P. Laurent (1992), Determining palaeostress orientations from faults and calcite twins: A case study near the Sainte-Victoire Range (southern France), *Tectonophysics*, *201*, 141–156, doi:10.1016/0040-1951(92)90180-E.

Leleu, S., J.-F. Ghienne, and G. Manatschal (2005), Upper Cretaceous-Palaeocene basin margin alluvial fans documenting interaction between tectonic and environmental processes (Provence, SE France), *Geol. Soc. Spec. Publ.*, *251*, 217–239.

Leleu, S., J.-F. Ghienne, and G. Manatschal (2009), Alluvial fan development and morphotectonic evolution in response to contractional fault reactivation (Late Cretaceous–Paleocene), Provence, France, *Basin Res.*, *21*, 157–187, doi:10.1111/j.1365-2117.2008.00378.x.

Macedo, J., and S. Marshak (1999), The geometry of fold-thrust belt salients, *Geol. Soc. Am. Bull.*, *111*, 1808–1822, doi:10.1130/0016-7606(1999)111<1808:COTGOF>2.3.CO;2.

Marshak, S., and M. S. Wilkerson (1992), Effect of overburden thickness on thrust belt geometry and development, *Tectonics*, *11*, 560–566, doi:10.1029/92TC00175.

Masse, J.-P. (1976), Les calcaires urgoniens de Provence (Valanginien-Aptien Inférieur) - Stratigraphie, paléontologie, paléoenvironnements et leur évolution, PhD thesis, 445 pp., Univ. de la Méditerranée, Aix-Marseille, France.

Masse, J.-P., and J. Philip (1976), Paléogéographie et tectonique du Crétacé moyen en Provence, *Rev. Geogr. Phys. Geol. Dyn.*, *2*, 49–66.

McClay, K. R. (1989), Analogue models of inversion tectonics, *Geol. Soc. Spec. Pub.*, *44*, 44–59.

McClay, K. R., and P. G. Buchanan (1992), Thrust faults in inverted extensional basins, in *Thrust Tectonics*, pp. 93–104, Chapman and Hall, London.

Meigs, A. J., and D. W. Burbank (1997), Growth of the south Pyrenean orogenic wedge, *Tectonics*, *16*, 239–258, doi:10.1029/96TC03641.

Ménard, G. (1980), Profondeur du socle antétriasique dans le Sud-Est de la France, *C. R. Acad. Sci. Paris*, *290*, 299–302.

Mitra, M. (2002), Fold-accommodation faults, *Am. Assoc. Pet. Geol. Bull.*, *86*, 671–693.

Molinaro, M., P. Leturmy, J.-C. Guezou, D. Frizon de Lamotte, and S. A. Eshraghi (2005), The structure and kinematics of the southeastern Zagros fold-thrust belt, Iran: From thin-skinned to thick-skinned tectonics, *Tectonics*, *24*, TC3007, doi:10.1029/2004TC001633.

Molliex, S., O. Bellier, M. Terrier, J. Lamarche, G. Martelet, and N. Espurt (2011), Tectonic and sedimentary inheritance on the structural framework of Provence (SE France): Importance of the Salon-Cavaillon fault, *Tectonophysics*, *501*, 1–16, doi:10.1016/j.tecto.2010.09.008.

Montenat, C., C. Hibsch, J.-C. Perrier, F. Pascaud, and P. de Bretizel (1997), Tectonique cassante d'âge Crétacé inférieur dans l'Arc de Nice (Alpes-Maritimes, France), *Geol. Alp.*, *73*, 59–66.

Mora, A., M. Parra, M. R. Strecker, A. Kammer, C. Dimaté, and F. Rodriguez (2006), Cenozoic contractional reactivation of Mesozoic extensional structures in the eastern cordillera of Colombia, *Tectonics*, *25*, TC2010, doi:10.1029/2005TC001854.

Mora, A., M. Parra, M. R. Strecker, E. R. Sobel, G. Zeilinger, C. Jaramillo, S. F. Da Silva, and M. Blanco (2010), The eastern foothills of the Eastern Cordillera of Colombia: An example of multiple factors controlling structural styles and active tectonics, *Geol. Soc. Am. Bull.*, *122*, 1846–1864, doi:10.1130/B30033.1.

Muñoz, J. A. (1992), Evolution of a continental collision belt: ECORS-Pyrenees crustal balanced cross-section, in *Thrust Tectonics*, pp. 235–246, Chapman and Hall, London, doi:10.1007/978-94-011-3066-0_21.

Price, R. A. (1986), The southeastern Canadian Cordillera: Thrust faulting, tectonic wedging, and delamination of the lithosphere, *J. Struct. Geol.*, *8*, 239–254, doi:10.1016/0191-8141(86)90046-5.

Ricour, J., I. Argyriadis, and R. Monteau (2005), Nouvelle interprétation tectonique de la montagne Sainte-Victoire (Provence, France), *C. R. Geosci.*, *337*, 1277–1283, doi:10.1016/j.crte.2005.07.005.

Roure, F., and B. Colletta (1996), Cenozoic inversion structures in the foreland of the Pyrenees and Alps, in *Peri-Tethys Memoir 2: Structure and Prospects of Alpine Basins and Forelands*, *Mem. du Mus. Natl. Hist. Nat.*, vol. 170, edited by P. A. Ziegler, pp. 173–209, Mus. Natl. Hist. Nat., Paris.

Rousset, C. (1978), De l'importance régionale de la faille d'Aix en Provence, *C. R. Acad. Sci. Paris*, *286*, 189–192.

Ruiz Barragan, M. R. (1978), Etude structural en Provence: Le Massif de la Sainte-Victoire, PhD thesis, 129 pp., Univ. Pierre et Marie Curie, Paris.

Said, A., D. Chardon, P. Baby, and J. Ouali (2011), Active oblique ramp faulting in the southern Tunisian atlas, *Tectonophysics*, *499*, 178–189, doi:10.1016/j.tecto.2011.01.010.

Saura, E., and A. Teixell (2006), Inversion of small basins: Effects on structural variations at the leading edge of the Axial Zone antiformal stack (Southern Pyrenees, Spain), *J. Struct. Geol.*, *28*, 1909–1920, doi:10.1016/j.jsg.2006.06.005.

Schettino, A., and E. Turco (2011), Tectonic history of the western Tethys since the Late Triassic, *Geol. Soc. Am. Bull.*, *123*, 89–105, doi:10.1130/B30064.1.

Shaw, J., C. Connors, and J. Suppe (2005), Seismic interpretation of contractional fault-related folds, AAPG seismic atlas, *Stud. Geol. Tulsa Okla.*, *53*, 1–156.

Suppe, J. (1983), Geometry and kinematics of fault-bend folding, *Am. J. Sci.*, *283*, 684–721, doi:10.2475/ajs.283.7.684.

Suppe, J., and D. A. Medwedeff (1990), Geometry and kinematics of fault-propagation folding, *Eclogae Geol. Helv.*, *83*(3), 409–454.

Suppe, J., T. T. Chou, and C. H. Stephen (1992), Rates of folding and faulting determined from growth strata, in *Thrust Tectonics*, edited by K. R. McClay, pp. 105–121, Chapman and Hall, New York, doi:10.1007/978-94-011-3066-0_9.

Tempier, C. (1972), *Les Faciès Calcaires du Jurassique Provençal*, *Trav. Lab. Sci. Terre, Sér. B*, vol. 4, pp. 1–371, Lab. Sci. Terr., Marseille, France.

Tempier, C. (1987), Modèle nouveau de mise en place des structures provençales, *Bull. Soc. Geol. Fr.*, *8*, 533–540.

Tempier, C., and J.-P. Durand (1981), Importance de l'épisode d'âge crétacé supérieur dans la structure du versant méridional de la montagne Sainte-Victoire (Provence), *C. R. Acad. Sci. Paris*, *293*, 629–632.

Terrier, M., O. Serrano, and F. Hanot (2008), Reassessment of the structural framework of western Provence (France): Consequence on the regional seismotectonic model, *Geodin. Acta*, *21*(5–6), 231–238, doi:10.3166/ga.21.231-238.

Toutin-Morin, N., and D. Bonijoly (1992), Structuration des basins de Provence orientale à la fin de l'ère primaire, *Cuad. Geol. Iber.*, *16*, 59–74.

Toutin-Morin, N., D. Bonijoly, C. Brocard, G. Dardeau, and M. Dubar (1992), Rôle des structures tardi à post-hercyniennes dans l'évolution de la plate-forme provençale (bordure des Maures et du Tanneron, France, *C. R. Acad. Sci. Paris*, *315*, 1725–1732.

Westphal, M., and J.-P. Durand (1990), Magnétostratigraphie des séries continentales fluviolacustres du Crétacé supérieur dans le synclinal de l'Arc (région d'Aix-en-Provence, France), *Bull. Soc. Geol. Fr.*, *8*, 609–620.